

# CASCADE: Cumulative Agentic Skill Creation through Autonomous Development and Evolution

Xu Huang<sup>1,2</sup>, Junwu Chen<sup>3,4\*</sup>, Yuxing Fei<sup>1,2</sup>, Zhuohan Li<sup>2</sup>,  
Philippe Schwaller<sup>3,4\*</sup>, Gerbrand Ceder<sup>1,2\*</sup>

<sup>1</sup>Department of Materials Science and Engineering, University of California, Berkeley, California, United States.

<sup>2</sup>Materials Sciences Division, Lawrence Berkeley National Laboratory, California, United States.

<sup>3</sup>Laboratory of Artificial Chemical Intelligence (LIAC), Institute of Chemical Sciences and Engineering, École Polytechnique Fédérale de Lausanne (EPFL), Lausanne, Switzerland.

<sup>4</sup>National Centre of Competence in Research (NCCR) Catalysis, École Polytechnique Fédérale de Lausanne (EPFL), Lausanne, Switzerland.

\*Corresponding author(s). E-mail(s): [junwu.chen@epfl.ch](mailto:junwu.chen@epfl.ch);  
[philippe.schwaller@epfl.ch](mailto:philippe.schwaller@epfl.ch); [gceder@berkeley.edu](mailto:gceder@berkeley.edu);

Contributing authors: [xu\\_huang@berkeley.edu](mailto:xu_huang@berkeley.edu); [yuxingfei@berkeley.edu](mailto:yuxingfei@berkeley.edu);  
[zhuohanli@lbl.gov](mailto:zhuohanli@lbl.gov);

## Abstract

Large language model (LLM) agents currently depend on predefined tools or brittle tool generation, constraining their capability and adaptability to complex scientific tasks. We introduce CASCADE, a self-evolving agentic framework representing an early instantiation of the transition from “LLM + tool use” to “LLM + skill acquisition”. CASCADE enables agents to master complex external tools and codify knowledge through two meta-skills: continuous learning via web search and code extraction, and self-reflection via introspection and knowledge graph exploration, among others. We evaluate CASCADE on SciSkillBench, a benchmark of 116 materials science and chemistry research tasks. CASCADE achieves a 93.3% success rate using GPT-5, compared to 35.4% without evolution mechanisms. We further demonstrate real-world applications in computational

analysis, autonomous laboratory experiments, and selective reproduction of published papers. Along with human-agent collaboration and memory consolidation, CASCADE accumulates executable skills that can be shared across agents and scientists, moving toward scalable AI-assisted scientific research.

## 1 Introduction

Tool use is not a unique ability of humans; what distinguishes humans is the cumulative acquisition of skills [1, 2]. Humans possess the unique ability to codify and accumulate know-how, recombining it into increasingly elaborate routines that can be taught, shared, and scaled [3]. Human technical culture advanced from opportunistic use of natural objects to the mastery of sophisticated inventions, a transition from tool use to skill acquisition. This shift enabled specialized expertise to accumulate and transmit across generations, sustaining division of labor and cooperation at scale [4, 5]. We argue that large language model (LLM) agents now stand at an analogous inflection point. Embracing this progression could offer a path toward self-evolving and adaptive agents [6, 7], thereby supporting truly autonomous and scalable agentic intelligence.

Under the prevailing “LLM + tool use” paradigm, most agents depend on custom-built wrappers predefined within a limited action space envisioned by humans [8, 9]. This confines their capabilities and hinders adaptation to complex tasks requiring novel tools for solving problems beyond predefined boundaries. The scalability of LLM agents across scientific domains remains limited, as each domain requires experts to curate detailed tool catalogs and tailored prompts (Fig. 1a, left). While recent efforts enable agents to generate tools autonomously, such tools typically rely solely on Python’s built-in libraries and remain simple and narrowly scoped [10, 11]. Furthermore, agents using external APIs, even when aided by web search or preselected resources, still lack mechanisms for skill mastery, human-in-the-loop collaboration, and memory-based consolidation [12–17]. As a result, such automated tool use remains brittle, limiting robustness and accuracy while bottlenecking self-evolution toward more capable skills.

As LLMs have become increasingly powerful in their reasoning and tool use capabilities, an expanding number of agentic systems focused on scientific discovery have emerged [18–25]. Most systems primarily excel at literature search, hypothesis generation, and data analysis [26–28], but lack robust capabilities for executing complex, long-horizon experiments, both computationally and physically. To function as true AI co-scientists, agents must possess autonomous execution capabilities that close the loop, enabling self-validation and iteration of ideas enhanced by tool implementation. Current efforts either rely on predefined tools [29, 30] or suffer from brittle tool generation [31–39], limitations widely acknowledged in the literature [14, 24, 40].

Here, we introduce CASCADE, an agentic framework facilitating AI co-scientists to develop cumulative executable skills. This framework represents an early instantiation of the transition from the “LLM + tool use” to “LLM + skill acquisition” paradigm, integrating multiple self-evolution mechanisms. Unlike traditional agentic systems that rely on problem-specific tools and prompts, CASCADE employs

general problem-solving methodologies and mindsets to cultivate two meta-skills, continuous learning and self-reflection, enabling inference-time evolution. Through natural language interfaces and multi-turn conversations, CASCADE lowers barriers to human-agent collaboration, allowing the agent to further evolve to solve more complex scientific problems. Additionally, it incorporates both session-wise memory, for referencing previous conversations, and consolidated memory, for retaining and retrieving key information, experience, and skill sets.

To evaluate CASCADE, we developed SciSkillBench, a comprehensive benchmark suite tailored for materials science and chemistry research. We conducted extensive baseline comparisons and ablation studies to validate CASCADE capabilities. We also evaluated CASCADE on specific research tasks, including determining materials' piezoelectricity and analyzing systematic differences in machine learning interatomic potentials (MLIPs) predictions [41] trained on different density functional theory (DFT) functionals [42]. Furthermore, we integrated CASCADE into an autonomous lab setting for real-world materials synthesis, characterization, and property measurement scenarios. CASCADE also successfully reproduced published results on Li intercalation voltages in rechargeable battery cathode materials [43]. These results demonstrate CASCADE's ability to master complex external tools, codify knowledge and skills, and build sophisticated, reusable routines for human scientists, other agents, and scientific platforms [37]. Importantly, CASCADE's only predefined tools are entirely domain-agnostic, containing no materials science or chemistry specific components, nor do prompts specify the use of any domain-specific tools. Through context engineering, this domain-agnostic design could enable rapid transfer to other fields requiring complex tool interaction, such as software engineering and biology [44, 45].

## 2 Results

### 2.1 CASCADE architecture

CASCADE is a self-evolving multi-agent system that serves as an AI co-scientist. In this study, we demonstrate its application in materials science and chemistry domains. It is an early example of the paradigm shift from “LLM + tool use” to “LLM + skill acquisition”. Through continuous learning, self-reflection, human-agent collaboration, and memory, CASCADE achieves self-evolution toward skill acquisition (Fig. 1a, right). These acquired skills are reusable by agents, human experts, and other systems.

As shown in Fig. 1b, CASCADE comprises an Orchestrator agent that coordinates multi-turn dialogues with human scientists through an interactive web interface ([Methods](#)). The system supports persistent session management, enabling users to initiate new conversations or resume previous sessions with full memory context. Upon receiving a user query, the Orchestrator retrieves relevant information from consolidated memory containing skill sets, user-specific preferences, API credentials, and accumulated experiences. The Orchestrator then selects between two problem-solving pathways. For straightforward queries or tasks solvable via adapted prior solutions, the Orchestrator uses the SimpleSolver for rapid response and resource efficiency ([Methods](#)). SimpleSolver generates code, manages dependencies, and executes the code in an isolated environment. Successful executions return results directly; errors trigger

escalation to DeepSolver. Complex problems bypass SimpleSolver entirely, proceeding directly to DeepSolver.

DeepSolver utilizes a four-step sequential workflow with conditional parallel debugging (Fig. 1c). Step 1: the Solution Researcher conducts web searches, extracts and retrieves code examples from URLs, and generates an initial code solution. Step 2: the Code Agent installs missing software dependencies, and executes the code, determining if debugging is needed. Step 3: If execution fails, three Debug Agent instances run concurrently, each employing different debugging strategies. Step 4: the Output Processor Agent evaluates all results, selects the best solution, and formats the output appropriately. Throughout the whole workflow, DeepSolver develops continuous learning and self-reflection meta-skills (Methods).

## 2.2 Evaluating DeepSolver on scientific computing tasks

DeepSolver is the key problem-solving engine that enables CASCADE to tackle real-world scientific research tasks. To rigorously assess its ability to autonomously solve such tasks without human intervention or memory access, we create SciSkillBench, a diverse, carefully curated benchmark of 116 tasks for materials science and chemistry research. SciSkillBench also provides a reusable and automated evaluation suite for other agentic systems.

As shown in Fig. 2a, SciSkillBench encompasses two primary types of tasks: (i) 76 data-oriented tasks, which include 22 data-retrieval problems, 24 data-analysis problems, 4 data-management problems, and 26 data-processing problems, and (ii) 40 computation-oriented tasks, which consist of 32 simulation problems and 8 specialized model and toolkit-related problems. For each of the six categories, we highlight the key databases, packages, and software utilized, along with examples of specific quantities that the tested system is required to acquire (Methods). Among them, 58 tasks are categorized as Level 0, which reflect scenarios where users can specify key functions or core procedural components, but prefer not to handle low-level implementation details or error recovery. The remaining 58 tasks are categorized as Level 1, in which only high-level objectives are provided, with limited procedural guidance, requiring greater autonomy from the agent. In summary, Level 0 and Level 1 tasks differ in how user queries are formulated, with Level 0 queries more closely resembling those posed by computational scientists and Level 1 queries resembling those typically posed by experimental scientists.

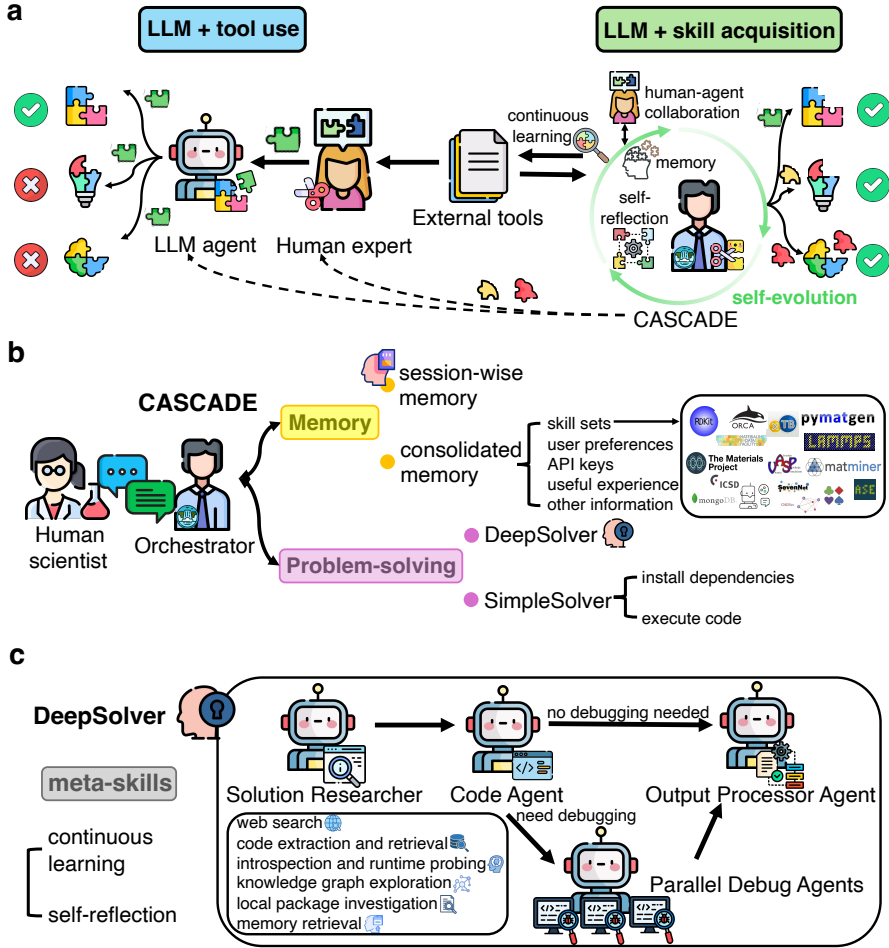


**Fig. 1** The “LLM + skill acquisition” paradigm and the CASCADE architecture. **a**, A puzzle-solving metaphor of the “LLM + tool use” versus the “LLM + skill acquisition” paradigm. On the left, agents rely on human experts to curate external tools. On the right, CASCADE showcases its ability to adeptly craft customized tools from complex external components, facilitating use by both human experts and LLM agents. **b**, The architecture of CASCADE. CASCADE facilitates multi-turn dialogues with human scientists through an interactive web interface, with persistent session management and consolidated memory in vector and graph databases. The Orchestrator agent within CASCADE selects between two solution pathways, the SimpleSolver or the DeepSolver, based on adaptable memory and task difficulty. **c**, DeepSolver architecture. DeepSolver coordinates four specialized agents that collaboratively solve complex tasks while autonomously acquiring new tools and skills. It follows a sequential workflow: the Solution Researcher generates the initial code solution; the Code Agent executes the code; if debugging is required, the Debug Agents intervene; and finally, the Output Processor Agent processes the results.

We benchmark the performance of DeepSolver on SciSkillBench against three baselines (Methods). The first baseline, referred to as Native, evaluates each LLM’s inherent capabilities without any self-evolution. In this scenario, the Solution Researcher generates code once, the Code Agent executes it once, and the Output Processor Agent

returns the result. The second baseline, designated as Search&Debug Baseline (S&D), reflects recent advancements in tool-making agents that enhance LLMs with capabilities such as web search and self-debugging, sometimes providing only one of these functions [10, 11, 13–17, 31–39]. In our implementation, we provide both search and debug functions to augment performance for this baseline. The Solution Researcher is enabled to conduct web search, while the Code Agent is required to engage in iterative self-debugging. For both of these baselines, as well as DeepSolver, we employ nine leading models as the LLMs for these multi-agent systems, with each agent utilizing the same LLM across the testing environment. These models include eight from OpenAI: GPT-5, GPT-5-mini, GPT-5-nano, O3, O4-mini, GPT-4.1, GPT-4.1-mini, and GPT-4.1-nano, in addition to one open-source model, Qwen3-Coder-30B-A3B-Instruct-FP8 (Qwen3-Coder-30B) [46]. For the third baseline, we implement a Claude Code agentic system leveraging Anthropic’s Claude Agent software development kit (SDK), which invokes Claude Code CLI with all its built-in tools, including web search and self-debugging capabilities. We select Claude-Sonnet-4.5, Anthropic’s highest-performing coding model at the time of testing, as the LLM for this system to probe the reach and limit of one of the strongest commercial coding agents on SciSkillBench.

For each of the above 28 agentic systems, we conduct three independent repetitions for each benchmark question (Methods). Table 1 presents the results for DeepSolver, Native, and S&D. It includes the overall success rate, the average run time, success rates for Level 0 and Level 1 questions, and pass@k accuracy (k=1, 2, 3) for all questions, Level 0, and Level 1. Here, pass@k accuracy means an answer is a “pass” if at least one of the first k responses is correct. From Table 1, we observe that CASCADE’s DeepSolver subsystem performs best across all comparisons. For nearly all agentic systems, the success rate for Level 0 questions consistently exceeds that for Level 1 questions. Even the most advanced models struggle without evolutionary mechanisms (Native), with the best overall success rate at only 35%. However, when models undergo effective evolution, particularly those models that can better understand our prompts and effectively utilize the general-purpose tools in DeepSolver, performance improvements are substantial. The highest overall success rate improvement is nearly 70% over Native with O3 model. For Level 0 tasks, the GPT-5, O3, and GPT-5-mini models achieve 100% pass@2 accuracy using DeepSolver. This suggests potential for handling more complex Level 0 research tasks. Furthermore, DeepSolver shows considerable enhancements over S&D across all models. The improvement with GPT-5 is relatively less pronounced, as some benchmark problems remain challenging, preventing accuracy from reaching 100%. This underscores the added value of CASCADE’s additional components in driving agents to further improve by incorporating memory and human-agent collaboration beyond DeepSolver’s inference-time self-evolution. Nevertheless, DeepSolver generally requires more time to output results.

For the Claude Code baseline, it achieves an average execution time of 238.50 seconds, with an overall success rate of 82.47%. The pass@k accuracy for all questions is 82.76%, 87.07%, and 87.93%, respectively. The success rate for Level 0 questions stands at 90.23%, with pass@k accuracy of 89.66%, 91.38%, and 93.10%, respectively. For Level 1 questions, the success rate is 74.71%, with pass@k accuracy of 75.86%, 82.76%, and 82.76%, respectively.

| Models                                   | Native S&D DeepSolver    |       |              | Native S&D DeepSolver    |       |               | Native S&D DeepSolver    |       |              | Native S&D DeepSolver |        |        |
|--|--------------------------|-------|--------------|--------------------------|-------|---------------|--------------------------|-------|--------------|-----------------------|--------|--------|
|  | Overall Success Rate (%) |       |              | 0-Level Success Rate (%) |       |               | 1-Level Success Rate (%) |       |              | Average Time (s)      |        |        |
|  | Pass@1                   |       |              | Pass@1                   |       |               | Pass@1                   |       |              |                       |        |        |
| GPT-5                                    | Pass@2                   |       |              | Pass@2                   |       |               | Pass@2                   |       |              |                       |        |        |
|  | Pass@3                   |       |              | Pass@3                   |       |               | Pass@3                   |       |              |                       |        |        |
|  | 35.36                    | 89.74 | <b>93.26</b> | 39.53                    | 94.71 | <b>96.47</b>  | 31.21                    | 84.80 | <b>90.06</b> | 240.42                | 503.54 | 587.84 |
| O3                                       | 32.76                    | 90.52 | <b>93.97</b> | 39.66                    | 94.83 | <b>96.55</b>  | 25.86                    | 86.21 | <b>91.38</b> |                       |        |        |
|  | 48.28                    | 93.97 | <b>97.41</b> | 55.17                    | 98.28 | <b>100.00</b> | 41.38                    | 89.66 | <b>94.83</b> |                       |        |        |
|  | 53.45                    | 94.83 | <b>98.28</b> | 60.34                    | 98.28 | <b>100.00</b> | 46.55                    | 91.38 | <b>96.55</b> |                       |        |        |
| O4-mini                                  | 23.05                    | 80.76 | <b>91.84</b> | 26.59                    | 85.88 | <b>97.70</b>  | 19.54                    | 75.72 | <b>85.80</b> | 153.01                | 352.31 | 406.65 |
|  | 21.55                    | 75.86 | <b>93.97</b> | 24.14                    | 79.31 | <b>96.55</b>  | 18.97                    | 72.41 | <b>91.38</b> |                       |        |        |
|  | 29.31                    | 89.66 | <b>98.28</b> | 34.48                    | 96.55 | <b>100.00</b> | 24.14                    | 82.76 | <b>96.55</b> |                       |        |        |
| GPT-5-mini                               | 35.34                    | 93.97 | <b>98.28</b> | 39.66                    | 98.28 | <b>100.00</b> | 31.03                    | 89.66 | <b>96.55</b> |                       |        |        |
|  | 24.71                    | 68.39 | <b>86.30</b> | 25.29                    | 75.29 | <b>86.63</b>  | 24.14                    | 61.49 | <b>85.96</b> | 118.08                | 177.46 | 248.11 |
|  | 24.14                    | 62.93 | <b>82.61</b> | 24.14                    | 67.24 | <b>84.48</b>  | 24.14                    | 58.62 | <b>80.70</b> |                       |        |        |
| GPT-4.1-mini                             | 34.48                    | 80.17 | <b>91.30</b> | 36.21                    | 86.21 | <b>91.38</b>  | 32.76                    | 74.14 | <b>91.23</b> |                       |        |        |
|  | 37.93                    | 84.48 | <b>94.78</b> | 39.66                    | 91.38 | <b>96.55</b>  | 36.21                    | 77.59 | <b>92.98</b> |                       |        |        |
|  | 22.09                    | 69.39 | <b>82.18</b> | 23.84                    | 76.07 | <b>89.08</b>  | 20.35                    | 62.87 | <b>75.29</b> | 353.26                | 469.28 | 452.75 |
| Gwen3-Coder<br>-30B-A3B<br>-Instruct-FP8 | 18.97                    | 71.55 | <b>83.62</b> | 20.69                    | 82.76 | <b>91.38</b>  | 17.24                    | 60.34 | <b>75.86</b> |                       |        |        |
|  | 30.17                    | 85.34 | <b>93.97</b> | 29.31                    | 91.38 | <b>100.00</b> | 31.03                    | 79.31 | <b>87.93</b> |                       |        |        |
|  | 34.48                    | 88.79 | <b>97.41</b> | 37.93                    | 93.10 | <b>100.00</b> | 31.03                    | 84.48 | <b>94.83</b> |                       |        |        |
| GPT-4.1                                  | 16.03                    | 45.65 | <b>72.78</b> | 18.24                    | 55.76 | <b>76.40</b>  | 13.87                    | 35.03 | <b>69.03</b> | 76.16                 | 156.23 | 190.05 |
|  | 15.52                    | 42.61 | <b>70.69</b> | 15.52                    | 51.72 | <b>74.14</b>  | 15.52                    | 33.33 | <b>67.24</b> |                       |        |        |
|  | 21.55                    | 59.13 | <b>85.34</b> | 24.14                    | 70.69 | <b>89.66</b>  | 18.97                    | 47.37 | <b>81.03</b> |                       |        |        |
| GPT-5-nano                               | 23.28                    | 64.35 | <b>89.66</b> | 27.59                    | 77.59 | <b>93.10</b>  | 18.97                    | 50.88 | <b>86.21</b> |                       |        |        |
|  | 21.41                    | 34.07 | <b>64.38</b> | 24.05                    | 42.75 | <b>72.14</b>  | 18.93                    | 25.90 | <b>57.24</b> | 425.72                | 515.41 | 599.19 |
|  | 20.87                    | 35.29 | <b>65.22</b> | 22.81                    | 41.18 | <b>70.69</b>  | 18.97                    | 29.41 | <b>59.65</b> |                       |        |        |
| GPT-4.1-nano                             | 30.43                    | 48.04 | <b>76.52</b> | 35.09                    | 56.86 | <b>81.03</b>  | 25.86                    | 39.22 | <b>71.93</b> |                       |        |        |
|  | 37.39                    | 52.94 | <b>80.00</b> | 43.86                    | 62.75 | <b>82.76</b>  | 31.03                    | 43.14 | <b>77.19</b> |                       |        |        |
|  | 19.83                    | 40.46 | <b>62.82</b> | 22.99                    | 47.67 | <b>71.68</b>  | 16.67                    | 33.33 | <b>54.02</b> | 67.20                 | 85.44  | 187.04 |
| GPT-4.1                                  | 18.97                    | 42.24 | <b>63.79</b> | 18.97                    | 46.55 | <b>67.24</b>  | 18.97                    | 37.93 | <b>60.34</b> |                       |        |        |
|  | 24.14                    | 55.17 | <b>74.14</b> | 29.31                    | 63.79 | <b>79.31</b>  | 18.97                    | 46.55 | <b>68.97</b> |                       |        |        |
|  | 27.59                    | 57.76 | <b>81.03</b> | 34.48                    | 67.24 | <b>87.93</b>  | 20.69                    | 48.28 | <b>74.14</b> |                       |        |        |
| GPT-5-nano                               | 16.95                    | 38.79 | <b>57.27</b> | 17.82                    | 40.80 | <b>60.82</b>  | 16.09                    | 36.78 | <b>53.76</b> | 145.70                | 196.05 | 394.24 |
|  | 16.38                    | 38.79 | <b>62.93</b> | 13.79                    | 37.93 | <b>63.79</b>  | 18.97                    | 39.66 | <b>62.07</b> |                       |        |        |
|  | 23.28                    | 49.14 | <b>75.00</b> | 24.14                    | 50.00 | <b>77.59</b>  | 22.41                    | 48.28 | <b>72.41</b> |                       |        |        |
| GPT-4.1-nano                             | 28.45                    | 61.21 | <b>81.90</b> | 32.76                    | 67.24 | <b>84.48</b>  | 24.14                    | 55.17 | <b>79.31</b> |                       |        |        |
|  | 6.38                     | 5.71  | <b>19.92</b> | 7.56                     | 3.57  | <b>24.60</b>  | 5.20                     | 7.88  | <b>15.38</b> | 51.91                 | 63.30  | 177.51 |
|  | 5.17                     | 6.03  | <b>22.81</b> | 5.17                     | 5.17  | <b>31.03</b>  | 5.17                     | 6.90  | <b>14.29</b> |                       |        |        |
| GPT-4.1-nano                             | 8.62                     | 9.48  | <b>30.70</b> | 8.62                     | 8.62  | <b>37.93</b>  | 8.62                     | 10.34 | <b>23.21</b> |                       |        |        |
|  | 12.07                    | 10.34 | <b>32.46</b> | 13.79                    | 8.62  | <b>39.66</b>  | 10.34                    | 12.07 | <b>25.00</b> |                       |        |        |

**Table 1 Baseline comparison across methods: Native, Search&Debug Baseline (S&D), and DeepSolver.** This table presents benchmark results for three different systems evaluated using a variety of models, with columns reflecting the overall success rate and the average time taken to produce results (in seconds). The success rates for Level 0 and Level 1 questions are shown separately, exhibiting each system’s performance in handling questions of varying complexity. The pass@k accuracy (k=1, 2, 3) metrics indicate the proportion of questions that are considered correct if at least one of the first k responses is accurate, reflecting system reliability and robustness. Bold text denotes the maximum success rates and pass@k accuracies for each model across the three systems (Native, S&D, DeepSolver).

To further investigate the performance advantages of DeepSolver’s self-evolution compared to the Native, S&D, and Claude Code baselines, we assess each system’s efficacy across two levels of task difficulty. Task difficulty is categorized using the P value which ranges from 0 to 1 [47]. This metric represents the proportion of correct responses generated among all models, with higher values indicating easier tasks. Specifically, tasks are classified as simple if the P value is greater than or equal to 0.5 and as difficult if it is less than 0.5 ([Methods](#)). Examples are provided in [Appendix B.1.3](#). In Fig. 2b, we illustrate each system’s pass@3 accuracy relative to task difficulty. It is clear that for the same LLM (indicated by the same color and marker shape), the accuracy achieved using the DeepSolver framework generally exceeds that of the Native and S&D baselines for both simple and difficult tasks. Notably, as task difficulty increases, the decline in pass@3 accuracy for DeepSolver is markedly less pronounced compared to the baselines. Claude Code (red star) demonstrates commendable performance on simple tasks but experiences a significant accuracy drop with increasing difficulty. These findings support the notion that DeepSolver has a superior ability to effectively handle complex tools, which is a crucial trait for a scientist co-pilot. In contrast, baseline systems exhibit a rapid performance decline, indicating bottlenecks in problem-solving. For example, Qwen3-Coder-30B with S&D shows a zero pass rate on difficult tasks. GPT-4.1-nano’s performance approaches zero across all three systems on difficult tasks. This is mainly due to the model’s limited ability to follow prompts and effectively utilize our designed tools, hindering its self-evolution capabilities.

In addition to conducting baseline comparisons, we perform ablation studies to assess the effects of removing each meta-skill from the DeepSolver system, specifically continuous learning and self-reflection, by removing corresponding tools and prompts ([Appendix B.2](#)). We observe varied contributions of the meta-skills across different language models. Notably, we find that in most cases, equipping the agentic system with the self-reflection meta-skill alone can outperform the conventional approach of combining both web search and self-debugging methods.

### 2.3 CASCADE in action: from computational reasoning to laboratory automation

Beyond benchmark performance, we evaluate CASCADE’s capabilities across four distinct real-world research scenarios, each demonstrating a different aspect of the skill acquisition paradigm. These applications span from pure computational reasoning tasks to physical laboratory automation, and from zero-shot problem solving to memory-enhanced collaborative research. Together, they illustrate how CASCADE transcends traditional tool use, moving toward a genuine scientific co-pilot capable of conducting end-to-end research workflows.

#### Automated scientific reasoning: piezoelectricity determination

This scenario demonstrates how CASCADE adeptly solves problems independently through DeepSolver, leveraging the OpenAI O3 model without relevant memory or human instruction. As displayed in Fig. 3a, CASCAD is tasked with determining

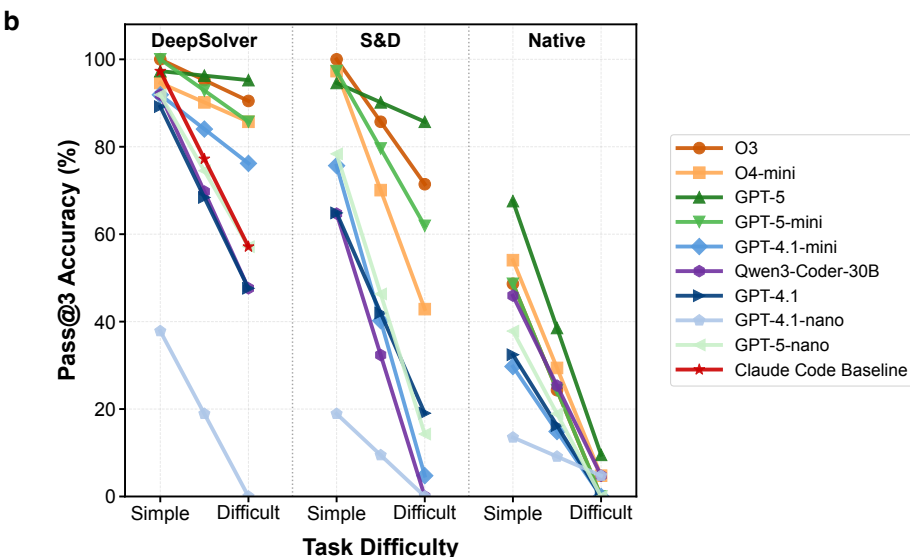
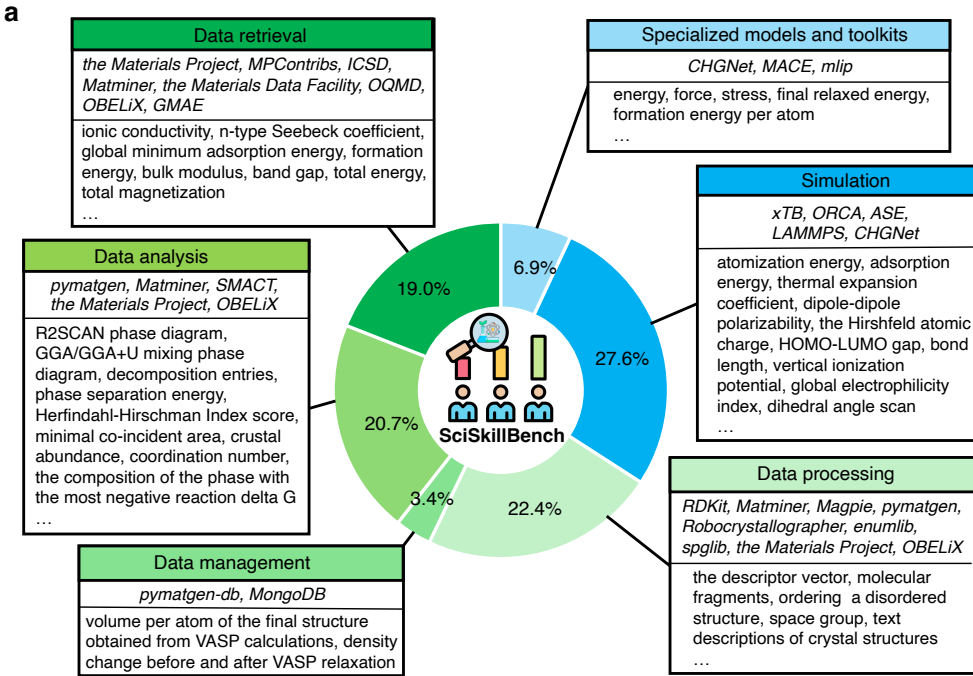


**Fig. 2 Task diversity in SciSkillBench and performance analysis. a,** Overview of the diverse tasks involved in SciSkillBench, comprising two main types: data-oriented tasks (76 in total) and computation-oriented tasks (40 in total). There are six specific categories with different proportions, namely: data retrieval (19.0%), data analysis (20.7%), data management (3.4%), data processing (22.4%), simulation (27.6%), and specialized models and toolkits (6.9%). The associated major databases, packages, and software for each category are listed, alongside examples of quantities that the benchmarked system is required to obtain. **b,** Pass@3 accuracy against task difficulty for DeepSolver, Search&Debug Baseline (S&D), Native, and Claude Code Baseline. Each backbone model is represented by a distinct color and marker shape. Claude Code Baseline (red star) is shown in the DeepSolver section. 9

whether a structure possesses piezoelectricity. We provide a JSON file named `structure.json` that contains a dictionary representation of a pymatgen [48] `Structure` object for this disordered structure. The agent succeeded on its first attempt, correctly identifying the structure's space group  $I4/mmm$ , point group  $4/mmm$ , and its centrosymmetric nature using pymatgen, ultimately concluding that the structure cannot exhibit piezoelectricity. Interestingly, in the code, it correctly takes point group 432 into account, which is non-piezoelectric though non-centrosymmetric [49], a detail that human scientists may overlook. This example demonstrates that when the agent has the ability to identify suitable external tools and robustly execute them, it can enhance its reasoning and yield reliable results.

### Hypothesis-driven discovery: predicting systematic errors in MLIPs

In Fig. 3b, CASCADE with the OpenAI O3 model is further evaluated with a task akin to the “Density prediction from MLIPs” section in a related article [50]. At the time of testing this task, the relevant content had not yet been published online. Specifically, CASCADE is asked to predict systematic differences between the GGA/GGA+U and  $r^2$ SCAN [51, 52] pretrained CHGNet models' predictions for density and volume per atom, where CHGNet is an MLIP [53]. Impressively, also on its first attempt, CASCADE formulated a correct hypothesis, validating it through experiments and subsequent data analysis (Appendix B.3).

### Laboratory automation: autonomous synthesis and characterization

To test whether CASCADE can contribute to the autonomous laboratory discovery loop beyond utilizing data and computation-related tools [54], we engage it in the complete workflow for the synthesis, characterization, measurement, and analysis of the compound  $\text{Li}_2\text{Fe}_{0.8}\text{Ni}_{0.2}\text{Cl}_4$ , as illustrated in Fig. 4. CASCADE, utilizing the OpenAI O3 model without previously relevant memory or human instruction, is tasked to interact with AlabOS [55], i.e., an operating system that orchestrates the experiment flows and provides an API interface for the users to submit experiments and check experiment status, and combine it with our in-house package, Alab-GPSS, that defines the workflows and helper functions to design experiments and submit to AlabOS. Since Alab-GPSS is proprietary software developed internally, it has not been included in the model training data, is not available online, and lacks any accompanying documentation. Thus, CASCADE has to learn how to use it on the fly by reading and interacting with the source code and file structures. After several attempts, CASCADE successfully submitted the job to the platform. To ensure laboratory safety, we verified the generated code before activating the autonomous lab devices. Notably, CASCADE successfully identified and utilized the appropriate functions, including `generate_recipe` for automatic stoichiometric balancing. However, the `generate_recipe` function itself still exhibited some issues during testing. Upon detecting the error, CASCADE intelligently implemented a fallback solution by performing stoichiometric calculations to ensure proper reaction balancing and successful task completion (Appendix B.3).

Following the measurement of the electrochemical impedance spectroscopy (EIS) for a sample with target composition of  $\text{Li}_2\text{Fe}_{0.8}\text{Ni}_{0.2}\text{Cl}_4$ , we proceeded to analyze the

**a**

 Determine whether the structure at the path read from `os.getenv('STRUCTURE_PATH')` has piezoelectricity.

 Because piezoelectricity requires the absence of an inversion center, a centrosymmetric crystal like this one cannot be piezoelectric. Therefore, the structure at the supplied path is NOT piezoelectric.

**b**

 Predict what systematic differences you expect between the GGA/GGA+U vs R2SCAN pretrained CHGNet models' predictions (after relaxation) for density and volume per atom compared to experimental values, and then prove your hypothesis with data and plots. You should use all the ICSD structures provided at the dataset path read from `os.getenv('ICSD_DATA_PATH')`.

**Hypothesis**

Because the default CHGNet model was trained on DFT data obtained with semi-local GGA/GGA+U functionals (mostly PBE-type), it should inherit the well-known GGA tendency to "over-estimate" equilibrium lattice parameters. A larger lattice gives

- higher volume per atom ( $V_{pa}$ )
- lower mass density ( $\rho$ )

mean  $\Delta \pm \sigma$  (predicted – experimental)

|  |                                  |
|--|----------------------------------|
| $\Delta V_{pa} (\text{\AA}^3/\text{atom})$ | $\Delta \rho (\text{g cm}^{-3})$ |
| GGA/GGA+U : $+0.248 \pm 0.311$             | $-0.099 \pm 0.110$               |
| R2SCAN : $+0.003 \pm 0.114$                | $-0.004 \pm 0.036$               |

Visual proof (files in `*chgnnet_icsd_analysis_outputs/*`)

- scatter\_volume\_per\_atom.png – both model predictions vs experiment. The R2SCAN dots sit almost on the diagonal, whereas GGA dots lie systematically above it.
- scatter\_density.png – similar for densities; GGA dots lie below the diagonal.
- hist\_delta\_volume\_per\_atom.png / hist\_delta\_density.png – histograms of the signed errors clearly show the GGA distribution shifted to positive  $\Delta V$  (negative  $\Delta \rho$ ) while the R2SCAN distribution is centered on 0.

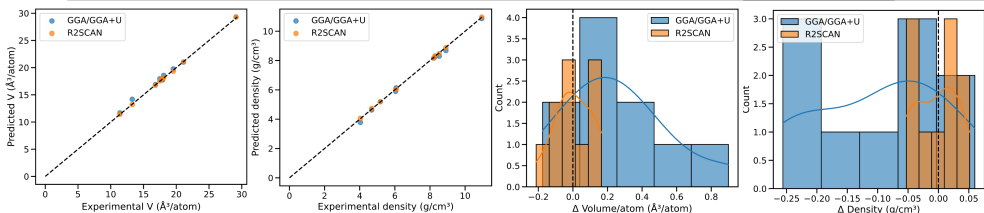


**Fig. 3** Piezoelectricity determination and prediction of machine learning interatomic potential systematic errors. **a**, Determining whether a structure exhibits piezoelectricity. Given this task, CASCADE executed the necessary code and reached the correct conclusion. **b**, Hypothesis formulation, experimental execution, and data analysis of systematic differences in density and volume per atom predictions using machine learning interatomic potentials trained on different density functional theory (DFT) functional data. CASCADE not only provided a reasonable and accurate solution but also generated compelling visualizations, with the four plots from left to right being: `scatter_volume_per_atom.png`, `scatter_density.png`, `hist_delta_volume_per_atom.png`, and `hist_delta_density.png`.

experimental data, which was provided to CASCADE to determine the ionic conductivity [56]. CASCADE successfully completed the task using the impedance package [57]. We then generated a Nyquist plot to visualize the quality of the data fitting [58]. Consequently, CASCADE's algorithm is approximately 60-fold faster and achieves a slightly higher coefficient of determination ( $R^2$ ; 0.991 compared with 0.989) than our existing solution code, yielding more accurate results. While we can continue to

improve our solution code manually, such improvements would require a considerable amount of time for parameter tuning (Appendix B.3).

Through these laboratory automation cases, we showcase CASCADE's ability to rapidly adapt and learn within a novel and customizable research environment, highlighting its potential as a scientific co-pilot. This capability ensures that agentic systems are not only impressive in demonstrations but also genuinely beneficial for diverse real-world applications.

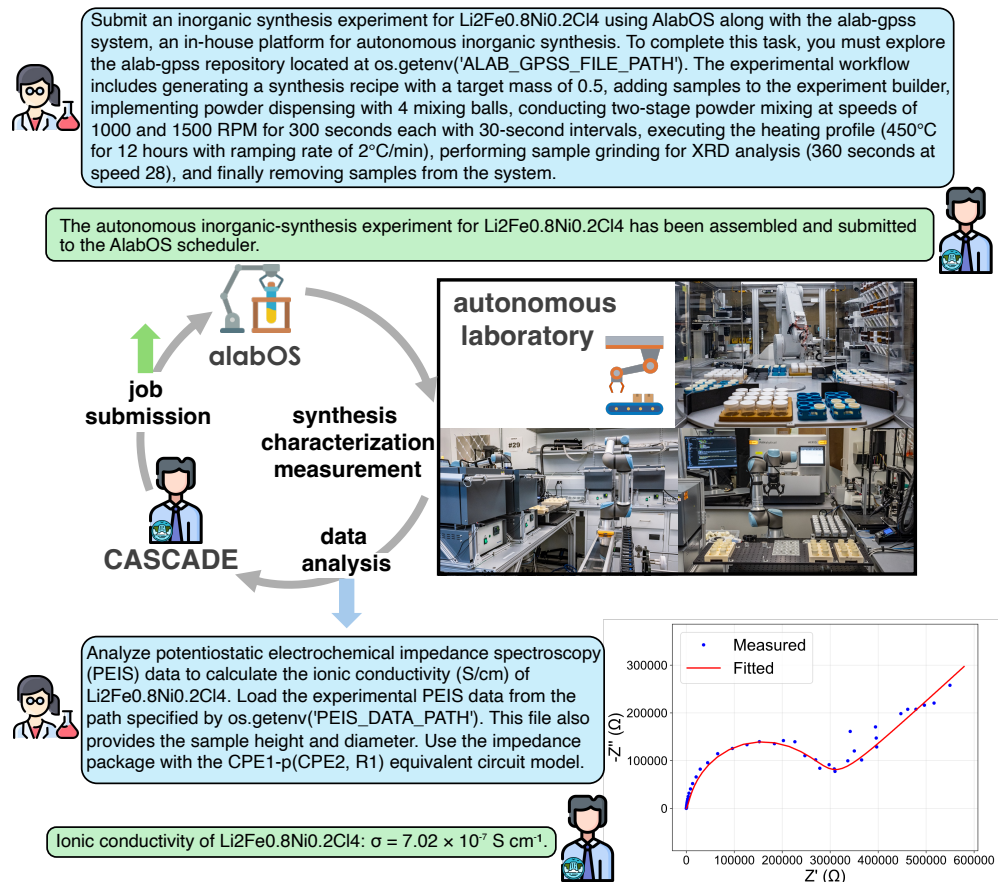


**Fig. 4 CASCADE integrated into the autonomous lab materials discovery loop.** CASCADE submitted the synthesis task for  $\text{Li}_2\text{Fe}_0.8\text{Ni}_0.2\text{Cl}_4$  to the autonomous lab (A-Lab) platform, allowing us to carry out the compound's synthesis, characterization, and electrochemical impedance spectroscopy (EIS) measurements. The acquired experimental data were fitted using CASCADE to determine the ionic conductivity. The bottom right corner shows a Nyquist plot visualizing the quality of the data fitting performed by CASCADE.

## Collaborative research with memory: reproducing published battery calculations

The above demonstrations primarily focus on CASCADE’s capability to learn new knowledge and master tools through DeepSolver, thereby enhancing its reasoning and problem-solving abilities. However, in addition to this inference-time self-evolution, human-agent collaboration and memory capabilities constitute vital components of CASCADE. These features enable CASCADE to evolve more rapidly, robustly, and reliably with guidance from human scientists and through the accumulation of skills, akin to the Compound Effect [59], ultimately allowing it to tackle more challenging problems. In the multi-turn interaction system, CASCADE, utilizing the OpenAI O3 model, is designed to promptly identify areas that require clarification or guidance from human scientists. In some cases, it is even able to detect inconsistencies in the questions posed by human scientists. As illustrated in Fig. 5a, we intentionally provide an incorrect material and Materials Project ID pairing; specifically, SiO2 is incorrectly assigned the ID mp-856. CASCADE directly point out this issue instead of mistakenly attempting to provide an erroneous answer.

Figure 5b demonstrates that when faced with more complex questions, CASCADE significantly benefits from human guidance, leading to improved problem resolution and effective storage of information in its memory. This collaborative process allows CASCADE to tackle more advanced queries through relevant memory retrieval, as shown in Fig. 5c. For this task, CASCADE is first asked to identify the MLIP we wish to employ from the Matbench Discovery leaderboard [60]. The task then involves calculating the average voltages over specified ranges:  $0 < x < 1$ ,  $0 < x < 0.5$ , and  $0.5 < x < 1$ , respectively, for Li\_xCoO2, utilizing MLIPs to obtain all energies after structural relaxation. Ultimately, CASCADE successfully reproduced the relevant contents from Fig. 2 of the referenced article [43] regarding Li\_xCoO2, as well as the content from its Fig. 4. The key difference is that, instead of employing four distinct DFT functionals for calculations, we utilize four MLIPs from SevenNet [61–63] to swiftly validate CASCADE’s capabilities (Appendix B.3).

## 3 Discussion

To enhance the effectiveness of LLM agents in assisting human scientific research, cultivating scientific reasoning is essential. Unlike text-based reasoning in mathematics and coding, scientific reasoning requires a deep understanding of complex external tools and their functionalities tailored to specific research objectives. This hands-on interaction with tools ensures that the agents’ reasoning is grounded, allowing them to refine and elevate their ideas through real-world experimentation. We introduce CASCADE, a self-evolving framework that cultivates and accumulates executable scientific skills. CASCADE represents an early embodiment of the dynamic and scalable “LLM + skill acquisition” paradigm, as opposed to the static and limited “LLM + tool use” paradigm. We also introduce SciSkillBench, a curated benchmark suite designed to fill the gap in evaluating agents’ or LLMs’ abilities to autonomously use a diverse range of tools for conducting materials science and chemistry research.



**Fig. 5 Human-agent collaboration with memory capability for reproducing published content.** **a**, Identification of issues in user queries. When asked to generate text descriptions with a mismatched material and Materials Project ID, CASCADe directly identified the problem and requested clarification. **b**, Calculation of average voltages. CASCADe computed the average voltages over specified ranges,  $0 < x < 1$  and  $0.5 < x < 1$ , for  $\text{Li}_x\text{CoO}_2$  during multi-turn interactions with users. **c**, Reproducing published work. CASCADe successfully calculated the average voltages over specified ranges for  $\text{Li}_x\text{CoO}_2$ , using four SevenNet models. Then, it generated plots similar to those in the referenced article. The bottom left plot is labeled average\_voltage\_models\_labeled.png, and the bottom right plot is average\_half\_voltage.png.

We systematically benchmark CASCADE’s key problem solver, DeepSolver, on SciSkillBench against three baselines and through ablation studies. DeepSolver achieves significantly higher accuracy with any tested LLM backbone and shows a slower performance decline as problem difficulty increases, indicating a stronger ability for inference-time self-evolution. We attribute these gains to two meta-skills: continuous learning and self-reflection, which balance agents’ plasticity and reliability. Additionally, we evaluate CASCADE’s performance in four real-world research scenarios. These demonstrations serve as proof-of-concept, showing that with thoughtful design, agents can autonomously traverse the end-to-end workflow, from literature search and hypothesis generation to experimental execution and data analysis, thus bridging the gap toward scientific reasoning through customizable computational and physical experiments.

Overall, CASCADE is designed to unlock the intelligence of LLMs by guiding them to adapt and evolve. In this process, they learn from up-to-date information, real-time failures, past experience, and human instructions. Notably, CASCADE is agnostic to specific research tools, questions, or scientific fields, facilitating easy transferability. The DeepSolver subsystem can also be integrated into other agentic systems to assist in skill creation and problem-solving.

The end-to-end agentic workflow reduces reliance on human input and grants agents greater freedom for autonomous exploration. However, it is still distant from achieving autonomous end-to-end discovery with truly novel insights. To achieve this goal, agents should iterate within this loop like human scientists, using trial and error along with optimization algorithms. As experience, data, and attempts accumulate, new discoveries may emerge.

To achieve long-horizon workflow iterations for new discoveries, the workflows agents create must be flexible and robust. To enhance systems like CASCADE, a promising direction is to explore efficient human-agent collaboration modes and improve agents’ memory capabilities, ensuring they can develop complicated yet reliable workflows. Another avenue is to strengthen the model’s inherent capabilities. While methods are documented in the literature, significant gaps remain between these theoretical descriptions and the practical challenges encountered during experiment execution. This hinders agents’ ability to reproduce previous work, let alone address new research questions without established references. Collecting data on how scientists approach simulation and experimental details in problem-solving would be valuable. This information could enhance agents’ abilities to execute and validate their ideas. Additionally, the complexity of research tasks and the flexibility in crafting tools could create challenges in identifying optimal tools and their appropriate application sequence within workflows, necessitating future investigation [64].

Furthermore, skills developed within CASCADE or future frameworks can serve as learnable external tools shared by scientific discovery agents and human scientists, breaking down temporal and spatial barriers to collaboration. Based on this, more efforts could focus on facilitating flexible cooperation between agents and humans at a larger scale. Such initiatives could foster a collaborative community for scaling scientific discovery, enabling the accumulation, transmission, and redeployment of wisdom, thereby facilitating evolution from the individual to the collective level.

## 4 Methods

### 4.1 CASCADE architecture

#### 4.1.1 MCP servers and tools

Our system leverages four specialized Model Context Protocol (MCP) servers to provide comprehensive capabilities for web search, code research and introspection, code execution and workspace management, as well as memory consolidation and retrieval. These servers comprise the third-party Tavily MCP server alongside three custom-developed servers: the memory server, research server, and workspace server. Through these servers, agents gain access to 15 tools for problem-solving: `save_to_memory`, `search_memory`, `tavily-search`, `extract_code_from_url`, `retrieve_extracted_code`, `check_installed_packages`, `install_dependencies`, `execute_code`, `quick_introspect`, `runtime_probe_snippet`, `parse_local_package`, `query_knowledge_graph`, `execute_shell_command`, `create_and_execute_script`, `read_file`. In addition to MCP server interfaces, we provide equivalent direct function implementations that bypass MCP protocol overhead. See [Appendix A](#) for detailed descriptions of each MCP server and tool, as well as the underlying principles of our architecture design, which draws inspiration from how human scientists approach learning new tools and acquiring domain-specific skills.

#### 4.1.2 Conversational system with memory and tracing

The conversational system built with Streamlit serves as the human-agent natural language interface of CASCADE. Users authenticate via Supabase Auth, and all memory operations are scoped to individual user identifiers to maintain personalized knowledge bases across sessions. The system implements a feedback mechanism that allows users to indicate satisfaction (which triggers memory preservation), request improvements, continue with follow-up questions, or terminate the current problem-solving cycle.

For session-wise memory, multi-turn conversation state is maintained through a session management layer utilizing `SQLiteSession` from the OpenAI Agents SDK, which automatically persists dialogue history across multiple conversation turns. Users can bookmark important sessions by toggling a saved status, assign custom titles for easy identification, and attach notes.

For consolidated memory, the Orchestrator agent within CASCADE is able to use `save_to_memory` and `search_memory` when needed, and agents inside DeepSolver can use `search_memory` when they are generating solutions.

The Orchestrator agent functions as the central controller, employing a structured decision-making workflow. Upon receiving a user query, the Orchestrator first retrieves relevant memories including past solutions, user preferences, and domain-specific knowledge. It then evaluates query completeness and coherence. If critical information is missing or the request appears ambiguous, it directly prompts the user for clarification before proceeding. Once the query is deemed complete, the Orchestrator determines whether the problem should be handled by the SimpleSolver pathway

(for straightforward tasks or those with high-confidence memory matches) or delegated to DeepSolver (for complex research or when SimpleSolver fails).

For observability and debugging, the system integrates MLflow [65] tracing to automatically record complete agent execution hierarchies. Each conversation turn generates a trace capturing the Orchestrator’s actions such as memory storage and search, package installation and code execution, and DeepSolver invocation. When DeepSolver is invoked, the trace records the full internal workflow, including all agent phases and their respective inputs, outputs, execution times, and tool call details.

#### 4.1.3 SimpleSolver

SimpleSolver represents a quick solution pathway within the Orchestrator agent rather than a separate agent architecture. When the Orchestrator determines that a problem is straightforward or can be confidently addressed by adapting relevant solutions from memory, it directly executes the solution without invoking DeepSolver. The Orchestrator writes code based on its knowledge or adapted memory matches, then uses `check_installed_packages` to verify package availability, `install_dependencies` to install any missing packages, and `execute_code` to run the solution. If execution succeeds, the Orchestrator answers the user’s question based on the results. If execution fails, the problem is delegated to DeepSolver for comprehensive research and iterative debugging.

#### 4.1.4 DeepSolver

Each agent in DeepSolver leverages specific MCP servers or direct tools to accomplish their specialized tasks within the collaborative workflow.

**Solution Researcher** initiates the workflow by conducting comprehensive research to generate initial code solutions for the user query. It is designed to perform a systematic research process that typically involves: understanding the request, searching relevant memory using `search_memory`, searching for relevant information using `tavily-search` with advanced search parameters, identifying required software if not specified, extracting code examples from identified URLs using `extract_code_from_url`, reviewing and understanding additional requirements, and synthesizing the final solution. The agent uses `retrieve_extracted_code` for vector-based similarity search when the extracted content is overwhelming, and optionally employs `quick_introspect` to confirm exact import paths and class/method/function names. For complex problems without explicit step-by-step instructions, it is designed to plan and decompose tasks, select appropriate tools to achieve objectives, and learn how to use them effectively. The output includes the user identifier for memory search, original user query, required packages list, and complete code solution.

**Code Agent** receives the initial solution and executes it. It can optionally use `search_memory` to find relevant memory. It is designed to perform a five-step execution process: analyzing input, verifying solution requirements using research tools (`tavily-search`, `extract_code_from_url`, `retrieve_extracted_code`) if needed, managing packages through `check_installed_packages` and `install_dependencies`, executing code using `execute_code`, and evaluating results to determine if debugging is needed. The agent is asked to execute code exactly once

without retries or self-debugging. The output includes the user identifier, original user query, executed code, execution output, and a boolean flag indicating whether debugging is needed.

**Debug Agent** instances run in parallel when the initial solution fails. The agents can optionally use `search_memory` to find relevant memory. They employ multiple debugging approaches after analyzing the error: Direct Fix for obvious errors; Introspection/Probe Fix using `quick_introspect` for import diagnostics and class/method/function discovery, and `runtime_probe_snippet` for resolving Key-Error and AttributeError; Knowledge Graph Fix using `check_package_version`, `parse_local_package`, and `query_knowledge_graph`, which serves as the global exploration layer when Introspection/Probe Fix does not resolve the issue; Local Package Fix using `execute_shell_command` and `create_and_execute_script` to locate relevant files, and `read_file` for examining specific files such as package source code and simulation output files; Research Fix using `tavily-search`, `extract_code_from_url`, and `retrieve_extracted_code` for finding documentation and solutions, especially for non-Python command-line tools invoked via subprocess; Diagnostic Fix for writing diagnostic code to investigate error causes; and Result Processing Fix for modifying code to produce complete and processable results. The agents use `execute_code` to test fixes, and `check_installed_packages` and `install_dependencies` for package management. Each agent is encouraged to combine and flexibly employ different debugging approaches to maximize the likelihood and efficiency of successful problem resolution.

**Output Processor Agent** evaluates all available results and generates the final response. When debugging is needed, the agent receives three debug results and evaluates each based on successful execution, presence of required data, and quality of results. It then selects the best result, with preference given to identical outputs from multiple debug agents as they are more likely to be correct. When no debugging is needed, it processes the successful execution result directly. The output includes original user query, success status, final code, execution results, and processed output, where processed output contains the answer and analysis that addresses the user's query.

**Meta-skills and memory system** Through carefully designed prompts for general problem-solving, DeepSolver develops continuous learning via the web search API and custom-built code extraction and retrieval tools. Self-reflection, another meta-skill, emerges through tools for code introspection, runtime probing, knowledge graph exploration, local package investigation, among others, extending beyond basic self-debugging. All agents, including the Solution Researcher, Code Agent, and Debug Agents, share access a consolidated memory. These combined capabilities produce human-like problem-solving behavior.

## 4.2 Benchmark Evaluation of DeepSolver

### 4.2.1 Benchmark tasks

SciSkillBench spans two principal categories: 76 data-oriented tasks and 40 computation-oriented tasks. Data tasks comprise (i) 22 data-retrieval problems from

resources such as the Materials Project [66], the Inorganic Crystal Structure Database (ICSD) [67], Matminer [68], MPCContribs [69], the Materials Data Facility [70], OQMD[71], OBELiX [72] and GMAE [73–75]; (ii) 24 data-analysis problems that use packages and databases including pymatgen [48, 76–79], Matminer, SMACT [80], the Materials Project and OBELiX; (iii) 4 data-management problems with pymatgen-db [81] and MongoDB [82]; and (iv) 26 data-processing problems that rely on RDKit [83], Matminer, Magpie [84], Robocrystallographer [85], pymatgen, enumlib [86–89], spglib [90], the Materials Project and OBELiX. Computation tasks include (v) 32 simulation problems with xTB [91], ORCA [92], ASE [93], LAMMPS [94] and CHGNet [53], together with (vi) 8 problems involving specialized models and toolkits such as CHGNet, MACE [95] and mlip [96].

The problems range from straightforward code adaptation and snippet stitching to undocumented queries that require strong scientific reasoning and exploratory coding, interaction with newly released packages or datasets absent from most model pre-training corpora, and navigation of outdated or misleading online documentation that can confuse agents. Many of these problems involve multiple external tools or different functions within a single tool, thus testing the agent’s ability to effectively identify and chain these tools/functions to solve the problems. More detailed examples of the benchmark tasks can be found in [Appendix B.1](#), where we provide some SciSkillBench instances as well as additional tasks not included in SciSkillBench.

#### 4.2.2 Baselines

For the three baselines, Native’s Solution Researcher operates without any tools and is designed to generate the code solution based solely on the knowledge of the underlying LLM. The Code Agent has access to `execute_code`, `check_installed_packages`, and `install_dependencies` to execute the code solution proposed by the Solution Researcher exactly once without debugging. Subsequently, the Output Processor Agent processes these results for automatic benchmark evaluation. In the S&D baseline, the Solution Researcher is enabled to conduct web searches through `tavily-search`, while the Code Agent performs iterative self-debugging using `execute_code`, `check_installed_packages`, and `install_dependencies`. The Claude Code baseline operates within Docker containers that reset after each run to ensure complete independence between test executions. Built on the Claude Agent SDK, this baseline grants the agent full access to Claude Code’s built-in capabilities, including file operations, code execution, and web search.

#### 4.2.3 Independent benchmark tests

For the evaluation of CASCADE, the three baselines, and the two ablation studies, we conducted independent benchmark tests across 46 system configurations. For each of the 116 benchmark tasks, we performed three independent repetitions per system configuration, resulting in a total of 16,008 experiments. To ensure complete isolation between experiments, each experiment was executed in a separate Python subprocess, and we cleared the Supabase database storing previously extracted code information and removed temporary files generated by agents from the previous experiment. Additionally, memory-based tools were disabled for all benchmark systems. For

experiments using OpenAI’s GPT-5, GPT-5-mini, and GPT-5-nano models with the OpenAI Agents SDK, we configured the reasoning effort to “medium” and verbosity to “low” to balance accuracy against computational cost and latency. For experiments using open-source Qwen models, we deployed the models locally using vLLM with an OpenAI-compatible API interface [97].

For accuracy evaluation, each benchmark task specifies the required output format and unit, which are communicated to the agent as part of the query. The agent’s processed output is then automatically compared against the ground truth answer within a predefined tolerance threshold. We set tolerance values according to the nature of each task: deterministic operations such as data retrieval use stringent tolerances approaching exact match, while computational simulations that inherently exhibit numerical variability use tolerances within acceptable ranges for the specific research task. This outcome-based evaluation assesses whether the agent produces correct final answers, though it does not guarantee the correctness of every intermediate step in the solution process. In the accuracy calculations, we excluded a small number of workflow failures such as instances when the LLM outputs invalid JSON that results in parsing errors.

#### 4.2.4 Task difficulty

To stratify benchmark questions by difficulty, we employed the P value (Item Difficulty), which denotes the proportion of models that correctly solved each Level 1 question. For each model-question pair, a question was considered solved if at least one of three independent attempts produced the correct answer (pass@3 criterion). We computed P values across 28 model configurations. Tasks were classified as simple if  $P \geq 0.5$  and difficult if  $P < 0.5$ , yielding 37 Simple and 21 Difficult questions. Model performance was then evaluated separately for each difficulty category using pass@3 accuracy.

**Data availability.** SciSkillBench is available at Figshare (<https://doi.org/10.6084/m9.figshare.30924998>).

**Code availability.** The source code of CASCADE is available on GitHub at <https://github.com/CederGroupHub/CASCADE>.

**Acknowledgements.** This work was primarily funded and intellectually led by the U.S. Department of Energy, Office of Science, Office of Basic Energy Sciences, Materials Sciences and Engineering Division under Contract No. DE-AC0205CH11231 (Materials Project program KC23MP). The work was also supported by the computational resources provided by the Extreme Science and Engineering Discovery Environment (XSEDE), supported by National Science Foundation grant number ACI1053575; the National Energy Research Scientific Computing Center (NERSC), a U.S. Department of Energy Office of Science User Facility located at Lawrence Berkeley National Laboratory; and the Swift Cluster resource provided by the National Renewable Energy Laboratory (NREL). Integrating this agentic system into the autonomous lab materials discovery loop was supported by the U.S. Department of Energy, Office of Science, Office of Advanced Scientific Computing Research and Office of Basic Energy Sciences, Scientific Discovery through the Advanced Computing (SciDAC) program under the FORUM-AI project. J.C. and P.S. acknowledge support

from the NCCR Catalysis (grant number 225147), a National Centre of Competence in Research funded by the Swiss National Science Foundation. We sincerely thank all the researchers and developers who created and maintained the datasets, packages, and software tools utilized in this work.

**Author contributions.** X.H., J.C. and P.S. conceived the initial idea. X.H. designed and developed the agentic system CASCADE. X.H. and J.C. curated the benchmark SciSkillBench; J.C. contributed xTB- , ASE- and ORCA-based tasks, while X.H. contributed the remaining tasks. X.H. benchmarked CASCADE’s DeepSolver against three baselines, conducted ablation studies, and performed additional evaluations of CASCADE. During the evaluation, Y.F. provided guidance on integrating CASCADE into the autonomous laboratory materials discovery loop, and Z.L. provided guidance on the average voltage calculation example. J.C., P.S., and G.C. offered insights and guidance throughout the project. All authors contributed to discussions and approved the final manuscript.

**Competing interests.** The authors declare no competing interests.

# Appendix

## Table of Contents

|          |  |           |
|----------|--|-----------|
| <b>A</b> | <b>CASCADE architecture</b>                      | <b>23</b> |
| A.1      | MCP server infrastructure and tools              | 23        |
| A.2      | Underlying principles of the architecture design | 24        |
| <b>B</b> | <b>Benchmark Evaluation of DeepSolver</b>        | <b>25</b> |
| B.1      | Benchmark tasks                                  | 25        |
| B.2      | Ablation studies                                 | 31        |
| B.3      | Demonstrations                                   | 32        |

## A CASCADE architecture

### A.1 MCP server infrastructure and tools

CASCADE leverages four specialized Model Context Protocol (MCP) servers to provide comprehensive capabilities for web search, code research and introspection, code execution and workspace management, as well as memory consolidation and retrieval.

#### Tavily MCP server

We use `tavily-search`, a search engine designed for AI agents, through the Tavily MCP server to provide real-time web search capabilities, enabling agents to discover relevant documentation, code examples, and implementation resources.

#### Memory server

Memory server employs `mem0` [98] configured with a hybrid dual-store architecture combining vector-based semantic search and graph-based entity-relationship storage. For semantic retrieval, memories are stored in a Supabase-hosted PostgreSQL database. A Neo4j graph database captures entity relationships, such as materials, properties, computational tools, API methods and functions, and their interconnections. Memory extraction utilizes GPT-4o-mini as the underlying language model. The server exposes two tools: `save_to_memory` and `search_memory`. The `save_to_memory` tool employs a dual-path strategy: first, the language model adds, updates, or deletes memory guided by custom prompts for both vector and graph stores; second, the complete original content is preserved verbatim in the vector store without language model processing, ensuring no information loss while maintaining efficient semantic searchability. The `search_memory` tool retrieves relevant memories from both stores, returning semantic matches from the vector store alongside entity relationships from the graph store.

#### Research server

Research server implements a sophisticated code intelligence and knowledge discovery system that provides comprehensive capabilities for web code extraction, agentic RAG (retrieval-augmented generation), code introspection, runtime probing, and knowledge graph construction and exploration.

**Code extraction and retrieval:** The `extract_code_from_url` tool implements intelligent web crawling with multi-strategy extraction capabilities and caching mechanisms using Supabase database storage. The tool supports both single-page extraction and smart crawling strategies that recursively follow internal links with intelligent fallback mechanisms. It automatically detects content types and applies specialized extractors for different documentation systems, including Jupyter notebooks, ReadTheDocs/Sphinx and MkDocs documentation, raw code files from repositories, and markdown content with intelligent parsing of fenced code blocks and command examples. It also extracts relevant text before and after code blocks using intelligent paragraph boundary detection, providing semantic context for code understanding. Optional LLM-generated summaries for extracted code are also available. The `retrieve_extracted_code` tool implements vector-based similarity search over extracted code blocks using embeddings with configurable match count.

**Code analysis:** The `quick_introspect` tool implements static-first analysis using Jedi [99] for import resolution and error diagnosis without runtime execution. The

tool provides comprehensive package, class, method, and function discovery with fuzzy matching capabilities. The `runtime_probe_snippet` tool provides ready-to-use code snippets for debugging runtime errors. When inserted at `KeyError` or `AttributeError` sites, these snippets display available keys/attributes, object type information, and similar name suggestions to help resolve these errors. The `parse_local_package` tool implements direct Neo4j knowledge graph construction from local Python packages using abstract syntax tree (AST) analysis. The tool extracts classes, methods, functions, attributes, and import relationships with detailed parameter information including type hints and default values. The `query_knowledge_graph` tool provides advanced querying capabilities for exploring repository structures, class hierarchies, method signatures, and code relationships in the knowledge graph using Cypher query language.

#### Workspace server

Workspace server provides a multi-environment code execution and management system. It supports `conda`, `venv`, and `uv` environments with cross-platform compatibility for Windows and Unix-like systems. The server prevents access to the directory containing benchmark tasks and results to avoid solution leakage and enforces security boundaries by confining all operations to the designated project root scope.

**Package management:** The `check_installed_packages` tool lists all installed packages in the current Python environment with version information and package count. The `install_dependencies` tool installs Python packages based on environment configuration. The `check_package_version` tool performs detailed package analysis including version detection, installation path resolution, and module location identification. The tool takes package names as input and handles name variations (hyphens, underscores, dots).

**Code execution:** The `execute_code` tool executes Python code in the configured environment. The tool saves code to temporary files in the code storage directory and executes with detailed output capture including `stdout` and `stderr`. The `execute_shell_command` tool executes shell commands with configurable working directory. The `create_and_execute_script` tool creates and executes shell scripts in the code storage directory.

**File operations:** The `read_file` tool reads content from text files. The `save_file` tool saves content to the designated directory for later reuse. In the CASCADE framework, however, the `save_file` tool is not utilized.

## A.2 Underlying principles of the architecture design

In designing CASCADE, we focused on how human scientists approach learning new tools and acquiring skills. Typically, they engage in deep thinking and experimentation to tackle problems, reflecting the role of the DeepSolver. This process may also involve discussions with others, akin to human-agent collaboration. Once they have mastered a new skill, they consolidate this experience into their memory.

Throughout the problem-solving process, much like DeepSolver, the first step is to act as Solution Researcher. Scientists perform online searches similar to those of agents using `tavily-search`. Their attention is directed towards key examples, paralleling

the use of tools such as `extract_code_from_url` and `retrieve_extracted_code`. Initially, they may verify the existence of certain imports, classes, methods, or functions in their code based on hints provided by some Integrated Development Environments (IDEs), similar to the `quick_introspect` tool we developed for agents to mitigate the common issue of hallucinations in LLMs [100].

After generating the initial solution, they move on to hands-on trials, which correspond to the tasks performed by the Code Agent. If errors arise, they engage in iterative refinements as Debug Agents would do. They start with local debugging approaches such as Introspection/Probe Fix, Direct Fix, or Diagnostic Fix. When these methods do not resolve the issue, they need to zoom out for broader rethinking and code exploration, employing Knowledge Graph Fix and Local Package Fix, and possibly continuing their online learning with Research Fix to deepen their understanding. After completing the task, they process and summarize the information to facilitate further consolidation, analogous to the Output Processor Agent.

During the tool and prompt design, we also consider context engineering to account for comprehensive situations, especially given that the agent’s performance may be inconsistent. For instance, when an agent fails to use a tool to achieve the desired outcome, a print message will remind the agent how to invoke the tool correctly or point out potential issues to consider. Additionally, it may suggest the next possible tool to use, such as `query_knowledge_graph` after `parse_local_package`.

## B Benchmark Evaluation of DeepSolver

### B.1 Benchmark tasks

#### B.1.1 SciSkillBench examples

Each benchmark task is defined as a JSON object with fields including `user_query`, `sources`, `input_type`, `output_type`, `answer`, `absolute_tolerance`, `unit`, `solution_code_or_process`, `reference_link`, `official_documentation`, and `notes`. In the examples below, we focus on the `user_query` field, which contains two difficulty levels: level 0 provides instructions with some function names, while level 1 presents a more concise query requiring the agent to determine the solution approach more independently.

##### 1. Straightforward code adaptation from the documentation

```
{  
  "user_query": {
```

```

    "0": "Use the InstaDeepAI mlip library to run batched inference
    with a pre-trained MACE model on aspirin. First, download the
    model and example data from HuggingFace using snapshot_download
    with repo_id='InstaDeepAI/MLIP-tutorials' and allow_patterns='
    simulation/*'. Then, load the pre-trained MLIP model using
    load_model_from_zip from 'simulation/example_model.zip', and
    run batched inference using run_batched_inference on the
    structures in 'simulation/aspirin_batched_example.xyz' with a
    batch size of 8. Finally, output the energy and forces for the
    1st structure (index starts at 0).",
    "1": "Use the InstaDeepAI mlip library to run batched inference
    with a pre-trained MACE model on aspirin. First, download the
    model and example data from HuggingFace using repo_id='
    InstaDeepAI/MLIP-tutorials' and allow_patterns='simulation/*'.
    Then, load the pre-trained MLIP model from 'simulation/
    example_model.zip', and run batched inference on the structures
    in 'simulation/aspirin_batched_example.xyz' with a batch size
    of 8. Finally, output the energy and forces for the 1st
    structure (index starts at 0)."
},
...
}

```

## 2. Undocumented queries

```

{
  "user_query": {
    "0": "What is the composition of the phase with the most negative
    reaction delta G (in kJ/mol) when Na2O and TiO2 react at 600K?
    Use pymatgen's GibbsComputedStructureEntry to help construct
    the phase diagram, and then use InterfacialReactivity to model
    an interface between Na2O and TiO2 to find all delta G of
    stable phases. Determine the one with the most negative delta G
    . Return a list in the order of composition string of the
    product phase and delta G value (in kJ/mol, rounded to 4
    decimal places).",
    "1": "What is the composition of the phase with the most negative
    reaction delta G (in kJ/mol) when Na2O and TiO2 react at 600K?
    In this process you must construct a suitable phase diagram and
    use pymatgen's built-in functionality to find the answer.
    Return a list in the order of composition string of the product
    phase and delta G value (in kJ/mol, rounded to 4 decimal
    places)."
},
...
}

```

```
{
  "user_query": {
    "0": "Give me the absolute error (meV/atom, rounded to four decimal
          places) of the formation energy per atom of Ti3AlC2 (mp-3747)
          predicted by the pretrained R2SCAN CHGNet model after relaxing
          the structures (keep all parameters as default), compared with
          the R2SCAN formation energy per atom that you query from the
          Materials Project through materials.thermo.search. Note that
          the CHGNet model does not provide built-in formation energy
          calculation method so you must find and relax all related
          structures and then calculate the formation energy per atom. To
          obtain the structures of constituent elements, you can use
          materials.thermo.search(chemsys=['Ti','Al','C'], is_stable=True
          , num_elements=(1,1), thermo_types=['R2SCAN'], fields=['
          material_id']) to get the material ids, and then use
          get_structure_by_material_id to fetch the structures for
          relaxation using the model loaded via CHGNet.load(model_name='
          r2scan'). Pay attention to the number of atoms in each
          structure, which is important for computing the formation
          energy per atom correctly.",
    "1": "Give me the absolute error (meV/atom, rounded to four decimal
          places) of the formation energy per atom of Ti3AlC2 (mp-3747)
          predicted by the pretrained R2SCAN CHGNet model after relaxing
          the structures (keep all parameters as default), compared with
          the R2SCAN formation energy per atom that you query from the
          Materials Project. Note that the CHGNet model does not provide
          built-in formation energy calculation method so you must find
          and relax all related structures and then calculate the
          formation energy per atom."
  },
  ...
}
```

3. Interaction with newly released packages or datasets absent from most model pre-training corpora

```
{
  "user_query": {
```

```

    "0": "Load the OBELiX dataset which comes from the paper titled
          OBELiX: A Curated Dataset of Crystal Structures and
          Experimentally Measured Ionic Conductivities for Lithium Solid-
          State Electrolytes, and then transform the first structure in
          the dataset to an ordered structure through the
          EnumerateStructureTransformation (picking the 1st one in the
          returned ranked list). Return to me a list in the order of the
          space group number of the original structure and the space
          group number of this ordered structure, using
          SpacegroupAnalyzer and get_space_group_number.",
    "1": "Load the OBELiX dataset which comes from the paper titled
          OBELiX: A Curated Dataset of Crystal Structures and
          Experimentally Measured Ionic Conductivities for Lithium Solid-
          State Electrolytes, and then transform the first structure in
          the dataset to an ordered structure through the
          EnumerateStructureTransformation (picking the 1st one in the
          returned ranked list). Return to me a list in the order of the
          space group number of the original structure and the space
          group number of this ordered structure."
  },
  ...
}

```

#### 4. Navigation of outdated or misleading online documentation

At the time of writing, the pymatgen-db and Materials Project documentation contain out-of-sync code examples that may confuse agents when performing the following tasks.

```

{
  "user_query": {
    "0": "Write code to retrieve the matching entries from the
          Inorganic Crystalline Structure Database (ICSD) for the
          material with Materials Project ID mp-18767, using materials.
          provenance.get_data_by_id() and get the database_IDs. Return a
          list of strings each with the format 'icsd-<ID number>'.",
    "1": "Write code to retrieve the matching entries from the
          Inorganic Crystalline Structure Database (ICSD) for the
          material with Materials Project ID mp-18767. Return a list of
          strings each with the format 'icsd-<ID number>'.",
    ...
  }
}

```

```

    "0": "I have already inserted an entire directory of VASP runs
          into the MongoDB database. Please use pymatgen-db to get the
          volume per atom of the final structure from the calculation.
          First, use QueryEngine class to query the task_id, and then
          use get_structure_from_id to get the structure. Finally,
          calculate the volume per atom of the structure. You should NOT
          insert data into the database.",
    "1": "I have already inserted an entire directory of VASP runs
          into the MongoDB database. Please use pymatgen-db to get the
          volume per atom of the final structure from the calculation.
          You should NOT insert data into the database."
    ...
}

```

### B.1.2 Additional examples

These additional tasks involve downloading datasets from published papers for subsequent processing and analysis [50, 101, 102]. They were excluded from the main SciSkillBench evaluation due to practical limitations, such as "Too Many Requests" errors encountered when accessing dataset URLs. Nevertheless, we have verified that DeepSolver with the OpenAI O3 model is capable of completing these tasks successfully.

```

{
  "user_query": {
    "0": "Download the test dataset of the paper titled MACE-OFF:
          Transferable Short Range Machine Learning Force Fields for
          Organic Molecules. You can use requests.get with the url https
          ://www.repository.cam.ac.uk/bitstreams/cb8351dd-f09c-413f-921c
          -67a702a7f0c5/download. Then, load corresponding model
          mace_off (choose the small one) to get the potential energy of
          the structure with the chemical formula C19H22Cl2N4O2S in
          this dataset.",
    "1": "Download the test dataset of the paper titled MACE-OFF:
          Transferable Short Range Machine Learning Force Fields for
          Organic Molecules, and load corresponding model (choose the
          small one) to get the potential energy of the structure with
          the chemical formula C19H22Cl2N4O2S in this dataset."
    ...
}
{
  "user_query": {

```

```

    "0": "Download the MP-r2SCAN dataset from the link https://doi.org/10.6084/m9.figshare.28245650.v2, and then give me the total number of frame ids and the mean of energy per atom. Return in a list in the order of number of frame ids and mean of energy per atom. You can use requests.get with the url https://figshare.com/ndownloader/files/51832613 to download the json file which has the structure of {mp-id: {frame-id: {energy_per_atom: ... } } }.",  

    "1": "Download the MP-r2SCAN dataset from the link https://doi.org/10.6084/m9.figshare.28245650.v2, and then give me the total number of frame ids and the mean of energy per atom. Return in a list in the order of number of frame ids and mean of energy per atom."  

    ...  

}

```

### B.1.3 Examples of simple and difficult tasks

Task difficulty is categorized using the P value, also known as Item Difficulty, which ranges from 0 to 1. This metric represents the proportion of correct responses generated among all models during assessment, with higher values indicating easier tasks. Specifically, tasks are classified as simple if the P value is greater than or equal to 0.5 and as difficult if it is less than 0.5.

#### 1. Simple tasks

Calculate the atomization energy (unit: eV) of a nitrogen molecule using ASE package and its Effective Medium Potential (EMT) calculator.

Calculate the adsorption energy (in eV) of one nitrogen atom on a 3x3 FCC Cu(111) surface with three atomic layers and 10 angstrom vacuum layer using ASE package and its Effective Medium Potential (EMT) calculator. Do not fix any atoms during the structure optimization!

Count the total number of molecular fragments for 0Cc1ccccc1CN using RDKit with parameters (1,6) and the default functional groups file 'FunctionalGroups.txt' in RDKit.

Calculate the crustal abundance (unit: ppm) of Al2O3 based on the mass fraction of each element in the compound using pymatgen and SMACT packages.

#### 2. Difficult tasks

Please use ORCA software to calculate the Hirshfeld atomic charge (unit: e) of the nitrogen atom in hydrogen cyanide using the DFT method and Hirshfeld population analysis at B3LYP/6-31+G\* accuracy.

Please use xtb software to calculate global electrophilicity index (unit: eV) of acetyl chloride.

Please use xtb to perform a dihedral angle scan of H-C-C-H in the ethane molecule and output the difference between the maximum and minimum energies (unit: eV). Scan the dihedral angle from 60 degrees to 420 degrees with 72 steps, using force constant 0.05.

In the Li-Mn-O chemical system using R2SCAN calculations, give me the materials id list of the decomposition entries of the R2SCAN entry of LiMnO2 (mp-18767, exactly this mp-id) using pymatgen's built-in functionality `get_decomp_and_phase_separation_energy`.

## B.2 Ablation studies

We performed ablation studies to assess the effects of removing each meta-skill from the DeepSolver system, specifically continuous learning and self-reflection, by removing corresponding tools and prompts. For No Self-Reflection (NSR), we disable DeepSolver's self-reflection meta-skill by removing the `quick_introspect` tool from the Solution Researcher and eliminating Debug Agents entirely. The Code Agent is then required to execute the code solution only once, without any debugging. For No Continuous Learning (NCL), we disable DeepSolver's continuous learning meta-skill by removing the tools `tavily-search`, `extract_code_from_url`, and `retrieve_extracted_code`, along with their related prompts from the system.

As shown in Table 2, we present the success rate, pass@k accuracy, and average execution time for configurations excluding self-reflection (NSR) and continuous learning (NCL), along with the results for DeepSolver. We observe varied contributions of the meta-skills across different language models. For instance, some models, such as GPT-5, O3, O4-mini, GPT-5-mini, GPT-4.1, and GPT-5-nano, demonstrate a greater improvement in accuracy due to self-reflection compared to continuous learning. Conversely, models like GPT-4.1-mini, Qwen3-Coder-30B, and GPT-4.1-nano appear to benefit more from continuous learning; this discrepancy may stem from their relatively weaker capabilities in coding and debugging, alongside their proficiency in web search. Overall, DeepSolver, which integrates both meta-skills, consistently achieves the best performance. An exception is noted with GPT-4.1, which exhibits optimal performance in the absence of continuous learning. Through recorded agent tracing during the test executions, we discover that GPT-4.1 rarely utilizes search-related functionalities, despite having access to relevant tools and prompts. Consequently, the

introduction of continuous learning tools and prompts may act as extraneous interference, hampering the agentic system’s efficiency in problem-solving. Moreover, we note that for over half of the models, DeepSolver spent less average time than the NCL configuration while achieving better accuracy.

Comparing Table 1 and Table 2, we observe that among the nine models evaluated, six models exhibited an overall success rate for the NCL configuration that surpassed that of the S&D baseline. The remaining three models also demonstrated performance rates that were only slightly lower than S&D. This indicates that our approach within CASCADE, which fosters and enhances the agent’s mastery of meta-skills, especially self-reflection, is more effective than the conventional combination of both search and self-debugging methods.

### B.3 Demonstrations

Demonstration examples can be found at [https://github.com/CederGroupHub/CASCADE/tree/main/benchmark\\_tasks\\_and\\_results/demonstration/free\\_form\\_output](https://github.com/CederGroupHub/CASCADE/tree/main/benchmark_tasks_and_results/demonstration/free_form_output), including task files (with user queries), reference solution code, agent-generated answers, and associated figures.

| Models                                   | NSR NCL DeepSolver       |              |              | NSR NCL DeepSolver       |              |               | NSR NCL DeepSolver       |              |              | NSR NCL DeepSolver |        |        |
|--|--------------------------|--------------|--------------|--------------------------|--------------|---------------|--------------------------|--------------|--------------|--------------------|--------|--------|
|  | Overall Success Rate (%) |              |              | 0-Level Success Rate (%) |              |               | 1-Level Success Rate (%) |              |              | Average Time (s)   |        |        |
|  | Pass@1                   | Pass@1       | Pass@1       | Pass@2                   | Pass@2       | Pass@2        | Pass@3                   | Pass@3       | Pass@3       | Pass@3             | Pass@3 | Pass@3 |
| GPT-5                                    | 62.64                    | 85.37        | <b>93.26</b> | 67.82                    | 90.30        | <b>96.47</b>  | 57.47                    | 80.37        | <b>90.06</b> | 520.60             | 505.03 | 587.84 |
|  | 65.52                    | 82.61        | <b>93.97</b> | 68.97                    | 86.21        | <b>96.55</b>  | 62.07                    | 78.95        | <b>91.38</b> |                    |        |        |
|  | 76.72                    | 90.43        | <b>97.41</b> | 75.86                    | 96.55        | <b>100.00</b> | 77.59                    | 84.21        | <b>94.83</b> |                    |        |        |
|  | 81.03                    | 91.30        | <b>98.28</b> | 82.76                    | 96.55        | <b>100.00</b> | 79.31                    | 85.96        | <b>96.55</b> |                    |        |        |
| O3                                       | 55.43                    | 86.02        | <b>91.84</b> | 60.69                    | 92.90        | <b>97.70</b>  | 50.00                    | 78.75        | <b>85.80</b> | 293.13             | 442.31 | 406.65 |
|  | 56.90                    | 84.35        | <b>93.97</b> | 62.07                    | 89.66        | <b>96.55</b>  | 51.72                    | 78.95        | <b>91.38</b> |                    |        |        |
|  | 66.38                    | 93.04        | <b>98.28</b> | 74.14                    | 96.55        | <b>100.00</b> | 58.62                    | 89.47        | <b>96.55</b> |                    |        |        |
|  | 70.69                    | 93.04        | <b>98.28</b> | 79.31                    | 96.55        | <b>100.00</b> | 62.07                    | 89.47        | <b>96.55</b> |                    |        |        |
| O4-mini                                  | 61.78                    | 73.59        | <b>86.30</b> | 65.52                    | 77.78        | <b>86.63</b>  | 58.05                    | 69.28        | <b>85.96</b> | 176.04             | 341.69 | 248.11 |
|  | 62.93                    | 75.00        | <b>82.61</b> | 70.69                    | 81.03        | <b>84.48</b>  | 55.17                    | 68.97        | <b>80.70</b> |                    |        |        |
|  | 68.97                    | 81.90        | <b>91.30</b> | 74.14                    | 87.93        | <b>91.38</b>  | 63.79                    | 75.86        | <b>91.23</b> |                    |        |        |
|  | 76.72                    | 84.48        | <b>94.78</b> | 79.31                    | 89.66        | <b>96.55</b>  | 74.14                    | 79.31        | <b>92.98</b> |                    |        |        |
| GPT-5-mini                               | 56.32                    | 66.97        | <b>82.18</b> | 60.34                    | 73.37        | <b>89.08</b>  | 52.30                    | 60.37        | <b>75.29</b> | 381.65             | 522.63 | 452.75 |
|  | 61.21                    | 62.28        | <b>83.62</b> | 67.24                    | 65.52        | <b>91.38</b>  | 55.17                    | 58.93        | <b>75.86</b> |                    |        |        |
|  | 73.28                    | 78.95        | <b>93.97</b> | 77.59                    | 87.93        | <b>100.00</b> | 68.97                    | 69.64        | <b>87.93</b> |                    |        |        |
|  | 76.72                    | 85.09        | <b>97.41</b> | 81.03                    | 94.83        | <b>100.00</b> | 72.41                    | 75.00        | <b>94.83</b> |                    |        |        |
| GPT-4.1-mini                             | 54.08                    | 46.52        | <b>72.78</b> | 64.02                    | 54.76        | <b>76.40</b>  | 44.31                    | 37.16        | <b>69.03</b> | 127.51             | 260.95 | 190.05 |
|  | 53.45                    | 40.71        | <b>70.69</b> | 65.52                    | 56.90        | <b>74.14</b>  | 41.38                    | 23.64        | <b>67.24</b> |                    |        |        |
|  | 62.93                    | 59.29        | <b>85.34</b> | 68.97                    | 75.86        | <b>89.66</b>  | 56.90                    | 41.82        | <b>81.03</b> |                    |        |        |
|  | 68.97                    | 70.80        | <b>89.66</b> | 74.14                    | 86.21        | <b>93.10</b>  | 63.79                    | 54.55        | <b>86.21</b> |                    |        |        |
| Qwen3-Coder<br>-30B-A3B<br>-Instruct-FP8 | 54.07                    | 30.10        | <b>64.38</b> | 60.83                    | 37.25        | <b>72.14</b>  | 47.62                    | 23.08        | <b>57.24</b> | 589.82             | 666.22 | 599.19 |
|  | 45.54                    | 32.17        | <b>65.22</b> | 52.73                    | 40.35        | <b>70.69</b>  | 38.60                    | 24.14        | <b>59.65</b> |                    |        |        |
|  | 66.07                    | 44.35        | <b>76.52</b> | 72.73                    | 52.63        | <b>81.03</b>  | 59.65                    | 36.21        | <b>71.93</b> |                    |        |        |
|  | 72.32                    | 46.09        | <b>80.00</b> | 78.18                    | 54.39        | <b>82.76</b>  | 66.67                    | 37.93        | <b>77.19</b> |                    |        |        |
| GPT-4.1                                  | 24.71                    | <b>72.06</b> | 62.82        | 27.01                    | <b>80.70</b> | 71.68         | 22.41                    | <b>63.31</b> | 54.02        | 39.35              | 153.36 | 187.04 |
|  | 26.72                    | <b>68.97</b> | 63.79        | 32.76                    | <b>77.59</b> | 67.24         | 20.69                    | <b>60.34</b> | 60.34        |                    |        |        |
|  | 31.03                    | <b>79.31</b> | 74.14        | 36.21                    | <b>84.48</b> | 79.31         | 25.86                    | <b>74.14</b> | 68.97        |                    |        |        |
|  | 32.76                    | <b>83.62</b> | 81.03        | 37.93                    | <b>89.66</b> | 87.93         | 27.59                    | <b>77.59</b> | 74.14        |                    |        |        |
| GPT-5-nano                               | 35.34                    | 42.06        | <b>57.27</b> | 40.80                    | 43.31        | <b>60.82</b>  | 29.89                    | 40.80        | <b>53.76</b> | 230.09             | 382.77 | 394.24 |
|  | 34.48                    | 38.37        | <b>62.93</b> | 39.66                    | 39.53        | <b>63.79</b>  | 29.31                    | 37.21        | <b>62.07</b> |                    |        |        |
|  | 44.83                    | 50.00        | <b>75.00</b> | 50.00                    | 53.49        | <b>77.59</b>  | 39.66                    | 46.51        | <b>72.41</b> |                    |        |        |
|  | 54.31                    | 54.65        | <b>81.90</b> | 56.90                    | 60.47        | <b>84.48</b>  | 51.72                    | 48.84        | <b>79.31</b> |                    |        |        |
| GPT-4.1-nano                             | 14.24                    | 12.89        | <b>19.92</b> | 15.48                    | 15.00        | <b>24.60</b>  | 13.04                    | 11.03        | <b>15.38</b> | 71.27              | 146.46 | 177.51 |
|  | 13.79                    | 8.93         | <b>22.81</b> | 13.79                    | 9.26         | <b>31.03</b>  | 13.79                    | 8.62         | <b>14.29</b> |                    |        |        |
|  | 19.83                    | 16.96        | <b>30.70</b> | 18.97                    | 18.52        | <b>37.93</b>  | 20.69                    | 15.52        | <b>23.21</b> |                    |        |        |
|  | 23.28                    | 17.86        | <b>32.46</b> | 25.86                    | 20.37        | <b>39.66</b>  | 20.69                    | 15.52        | <b>25.00</b> |                    |        |        |

**Table 2 Ablation study results: impact of meta-skills on DeepSolver’s performance.**

This table presents the benchmark results for different configurations of the DeepSolver system, specifically analyzing the effects of removing self-reflection (No Self-Reflection, NSR) and continuous learning (No continuous learning, NCL). It includes the success rates, pass@k accuracy (k=1, 2, 3), and average execution time (in seconds) for each configuration evaluated across various models. The pass@k accuracy metrics indicate the proportion of questions that are considered correct if at least one of the first k responses is accurate, reflecting system reliability and robustness. Bold text denotes the maximum success rates and pass@k accuracies for each model across the configurations.

## References

- [1] Goodall, J.: Tool-using and aimed throwing in a community of free-living chimpanzees. *Nature* **201**(4926), 1264–1266 (1964)
- [2] Pargeter, J., Khreisheh, N., Stout, D.: Understanding stone tool-making skill acquisition: Experimental methods and evolutionary implications. *Journal of Human Evolution* **133**, 146–166 (2019)
- [3] Stout, D., Hecht, E.E.: Evolutionary neuroscience of cumulative culture. *Proceedings of the National Academy of Sciences* **114**(30), 7861–7868 (2017)
- [4] Migliano, A.B., Vinicius, L.: The origins of human cumulative culture: from the foraging niche to collective intelligence. *Philosophical Transactions of the Royal Society B* **377**(1843), 20200317 (2022)
- [5] Tomasello, M.: *Becoming Human: A Theory of Ontogeny*. The Belknap Press of Harvard University Press, Cambridge, MA, USA (2019)
- [6] Gao, H.-a., Geng, J., Hua, W., Hu, M., Juan, X., Liu, H., Liu, S., Qiu, J., Qi, X., Wu, Y., et al.: A survey of self-evolving agents: On path to artificial super intelligence. *arXiv preprint arXiv:2507.21046* (2025)
- [7] Jiang, P., Lin, J., Shi, Z., Wang, Z., He, L., Wu, Y., Zhong, M., Song, P., Zhang, Q., Wang, H., et al.: Adaptation of agentic ai. *arXiv preprint arXiv:2512.16301* (2025)
- [8] Schick, T., Dwivedi-Yu, J., Dessim, R., Raileanu, R., Lomeli, M., Hambro, E., Zettlemoyer, L., Cancedda, N., Scialom, T.: Toolformer: Language models can teach themselves to use tools. *Advances in Neural Information Processing Systems* **36**, 68539–68551 (2023)
- [9] Qin, Y., Liang, S., Ye, Y., Zhu, K., Yan, L., Lu, Y., Lin, Y., Cong, X., Tang, X., Qian, B., et al.: Toolllm: Facilitating large language models to master 16000+ real-world apis. In: *The Twelfth International Conference on Learning Representations* (2024)
- [10] Cai, T., Wang, X., Ma, T., Chen, X., Zhou, D.: Large language models as tool makers. In: *The Twelfth International Conference on Learning Representations* (2024)
- [11] Yuan, L., Chen, Y., Wang, X., Fung, Y.R., Peng, H., Ji, H.: Craft: Customizing llms by creating and retrieving from specialized toolsets. (2024)
- [12] Chen, X., Lin, M., Schärli, N., Zhou, D.: Teaching large language models to self-debug. In: *The Twelfth International Conference on Learning Representations* (2024)

- [13] Qiu, J., Qi, X., Zhang, T., Juan, X., Guo, J., Lu, Y., Wang, Y., Yao, Z., Ren, Q., Jiang, X., et al.: Alita: Generalist agent enabling scalable agentic reasoning with minimal predefinition and maximal self-evolution. arXiv preprint arXiv:2505.20286 (2025)
- [14] Haque, M.A., Williams, J., Siddique, S., Islam, M.H., Ali, H., Gupta, K.D., George, R.: Advanced tool learning and selection system (atlass): A closed-loop framework using llm. arXiv preprint arXiv:2503.10071 (2025)
- [15] Wang, X., Li, B., Song, Y., Xu, F.F., Tang, X., Zhuge, M., Pan, J., Song, Y., Li, B., Singh, J., et al.: Openhands: An open platform for ai software developers as generalist agents. In: The Thirteenth International Conference on Learning Representations (2025)
- [16] Tang, J., Fan, T., Huang, C.: Autoagent: A fully-automated and zero-code framework for llm agents. arXiv preprint arXiv:2502.05957 (2025)
- [17] Zheng, B., Fatemi, M.Y., Jin, X., Wang, Z.Z., Gandhi, A., Song, Y., Gu, Y., Srinivasa, J., Liu, G., Neubig, G., et al.: Skillweaver: Web agents can self-improve by discovering and honing skills. arXiv preprint arXiv:2504.07079 (2025)
- [18] M. Bran, A., Cox, S., Schilter, O., Baldassari, C., White, A.D., Schwaller, P.: Augmenting large language models with chemistry tools. *Nature Machine Intelligence* **6**(5), 525–535 (2024)
- [19] Boiko, D.A., MacKnight, R., Kline, B., Gomes, G.: Autonomous chemical research with large language models. *Nature* **624**(7992), 570–578 (2023)
- [20] Ruan, Y., Lu, C., Xu, N., He, Y., Chen, Y., Zhang, J., Xuan, J., Pan, J., Fang, Q., Gao, H., et al.: An automatic end-to-end chemical synthesis development platform powered by large language models. *Nature communications* **15**(1), 10160 (2024)
- [21] Chai, J., Tang, S., Ye, R., Du, Y., Zhu, X., Zhou, M., Wang, Y., Zhang, Y., Zhang, L., Chen, S., et al.: Scimaster: Towards general-purpose scientific ai agents, part i. x-master as foundation: Can we lead on humanity’s last exam? arXiv preprint arXiv:2507.05241 (2025)
- [22] McNaughton, A.D., Sankar Ramalaxmi, G.K., Kruel, A., Knutson, C.R., Varikoti, R.A., Kumar, N.: Cactus: Chemistry agent connecting tool usage to science. *ACS omega* **9**(46), 46563–46573 (2024)
- [23] Huang, K., Zhang, S., Wang, H., Qu, Y., Lu, Y., Roohani, Y., Li, R., Qiu, L., Li, G., Zhang, J., et al.: Biomni: A general-purpose biomedical ai agent. biorxiv (2025)
- [24] Swanson, K., Wu, W., Bulaong, N.L., Pak, J.E., Zou, J.: The virtual lab of ai

agents designs new sars-cov-2 nanobodies. *Nature*, 1–3 (2025)

- [25] Takahara, I., Mizoguchi, T., Liu, B.: Accelerated inorganic materials design with generative ai agents. *arXiv preprint arXiv:2504.00741* (2025)
- [26] Skarlinski, M.D., Cox, S., Laurent, J.M., Braza, J.D., Hinks, M., Hammerling, M.J., Ponnnapati, M., Rodriques, S.G., White, A.D.: Language agents achieve superhuman synthesis of scientific knowledge. *arXiv preprint arXiv:2409.13740* (2024)
- [27] Ghareeb, A.E., Chang, B., Mitchener, L., Yiu, A., Szostkiewicz, C.J., Laurent, J.M., Razzak, M.T., White, A.D., Hinks, M.M., Rodriques, S.G.: Robin: A multi-agent system for automating scientific discovery. *arXiv preprint arXiv:2505.13400* (2025)
- [28] Mitchener, L., Yiu, A., Chang, B., Bourdenx, M., Nadolski, T., Sulovari, A., Landsness, E.C., Barabasi, D.L., Narayanan, S., Evans, N., et al.: Kosmos: An ai scientist for autonomous discovery. *arXiv preprint arXiv:2511.02824* (2025)
- [29] Zou, Y., Cheng, A.H., Aldossary, A., Bai, J., Leong, S.X., Campos-Gonzalez-Angulo, J.A., Choi, C., Ser, C.T., Tom, G., Wang, A., et al.: El agente: An autonomous agent for quantum chemistry. *Matter* **8**(7) (2025)
- [30] Chandrasekhar, A., Farimani, A.B.: Automating md simulations for proteins using large language models: Namd-agent. *arXiv preprint arXiv:2507.07887* (2025)
- [31] Villaescusa-Navarro, F., Bolliet, B., Villanueva-Domingo, P., Bayer, A.E., Acquah, A., Amancharla, C., Barzilay-Siegal, A., Bermejo, P., Bilodeau, C., Ramírez, P.C., et al.: The denario project: Deep knowledge ai agents for scientific discovery. *arXiv preprint arXiv:2510.26887* (2025)
- [32] Yao, L., Samantray, S., Ghosh, A., Roccapirore, K., Kovarik, L., Allec, S., Ziatdinov, M.: Operationalizing serendipity: Multi-agent ai workflows for enhanced materials characterization with theory-in-the-loop. *arXiv preprint arXiv:2508.06569* (2025)
- [33] Jin, R., Zhang, Z., Wang, M., Cong, L.: Stella: Self-evolving llm agent for biomedical research. *arXiv preprint arXiv:2507.02004* (2025)
- [34] Liu, S., Xu, J., Ye, B., Hu, B., Srolovitz, D.J., Wen, T.: Mattools: Benchmarking large language models for materials science tools. *arXiv preprint arXiv:2505.10852* (2025)
- [35] Wölflein, G., Ferber, D., Truhn, D., Arandjelovic, O., Kather, J.N.: Llm agents making agent tools. In: *Proceedings of the 63rd Annual Meeting of the Association for Computational Linguistics (Volume 1: Long Papers)*, pp. 26092–26130

(2025)

- [36] Miao, J., Davis, J.R., Zhang, Y., Pritchard, J.K., Zou, J.: Paper2agent: Reimagining research papers as interactive and reliable ai agents. arXiv preprint arXiv:2509.06917 (2025)
- [37] Gao, S., Zhu, R., Sui, P., Kong, Z., Aldogom, S., Huang, Y., Noori, A., Shamji, R., Parvataneni, K., Tsilgkaridis, T., et al.: Democratizing ai scientists using tooluniverse. arXiv preprint arXiv:2509.23426 (2025)
- [38] Orimo, Y., Kurata, I., Mori, H., Okuno, R., Sawada, R., Okanohara, D.: Parc: An autonomous self-reflective coding agent for robust execution of long-horizon tasks. arXiv preprint arXiv:2512.03549 (2025)
- [39] Zhou, L., Ling, H., Yan, K., Zhao, K., Qian, X., Arróyave, R., Qian, X., Ji, S.: Toward greater autonomy in materials discovery agents: Unifying planning, physics, and scientists. arXiv preprint arXiv:2506.05616 (2025)
- [40] Chen, Z., Chen, S., Ning, Y., Zhang, Q., Wang, B., Yu, B., Li, Y., Liao, Z., Wei, C., Lu, Z., et al.: Scienceagentbench: Toward rigorous assessment of language agents for data-driven scientific discovery. arXiv preprint arXiv:2410.05080 (2024)
- [41] Deringer, V.L., Caro, M.A., Csányi, G.: Machine learning interatomic potentials as emerging tools for materials science. *Advanced Materials* **31**(46), 1902765 (2019)
- [42] Geerlings, P., De Proft, F., Langenaeker, W.: Conceptual density functional theory. *Chemical reviews* **103**(5), 1793–1874 (2003)
- [43] Isaacs, E.B., Patel, S., Wolverton, C.: Prediction of li intercalation voltages in rechargeable battery cathode materials: Effects of exchange-correlation functional, van der waals interactions, and hubbard u. *Physical Review Materials* **4**(6), 065405 (2020)
- [44] Hua, Q., Ye, L., Fu, D., Xiao, Y., Cai, X., Wu, Y., Lin, J., Wang, J., Liu, P.: Context engineering 2.0: The context of context engineering. arXiv preprint arXiv:2510.26493 (2025)
- [45] Zhang, Q., Hu, C., Upasani, S., Ma, B., Hong, F., Kamanuru, V., Rainton, J., Wu, C., Ji, M., Li, H., et al.: Agentic context engineering: Evolving contexts for self-improving language models. arXiv preprint arXiv:2510.04618 (2025)
- [46] Yang, A., Li, A., Yang, B., Zhang, B., Hui, B., Zheng, B., Yu, B., Gao, C., Huang, C., Lv, C., et al.: Qwen3 technical report. arXiv preprint arXiv:2505.09388 (2025)

[47] Rezigalla, A.A., Eleragi, A.M.E.S.A., Elhussein, A.B., Alfaifi, J., ALGhamdi, M.A., Al Ameer, A.Y., Yahia, A.I.O., Mohammed, O.A., Adam, M.I.E.: Item analysis: the impact of distractor efficiency on the difficulty index and discrimination power of multiple-choice items. *BMC Medical Education* **24**(1), 445 (2024)

[48] Ong, S.P., Richards, W.D., Jain, A., Hautier, G., Kocher, M., Cholia, S., Gunter, D., Chevrier, V.L., Persson, K.A., Ceder, G.: Python materials genomics (pymatgen): A robust, open-source python library for materials analysis. *Computational Materials Science* **68**, 314–319 (2013)

[49] Gorfman, S., Zhang, N.: Piezoelectric coefficients and crystallographic symmetry. *Piezoelectric Materials: From Fundamentals to Emerging Applications* **1**, 1–15 (2024)

[50] Huang, X., Deng, B., Zhong, P., Kaplan, A.D., Persson, K.A., Ceder, G.: Cross-functional transferability in foundation machine learning interatomic potentials. *npj Computational Materials* **11**(1), 313 (2025)

[51] Perdew, J.P., Schmidt, K.: Jacob's ladder of density functional approximations for the exchange-correlation energy. In: *AIP Conference Proceedings*, vol. 577, pp. 1–20 (2001). American Institute of Physics

[52] Anisimov, V.I., Zaanen, J., Andersen, O.K.: Band theory and mott insulators: Hubbard  $u$  instead of stoner  $i$ . *Physical Review B* **44**(3), 943 (1991)

[53] Deng, B., Zhong, P., Jun, K., Riebesell, J., Han, K., Bartel, C.J., Ceder, G.: Chgnet as a pretrained universal neural network potential for charge-informed atomistic modelling. *Nature Machine Intelligence* **5**(9), 1031–1041 (2023)

[54] Szymanski, N.J., Rendy, B., Fei, Y., Kumar, R.E., He, T., Milsted, D., McDermott, M.J., Gallant, M., Cubuk, E.D., Merchant, A., *et al.*: An autonomous laboratory for the accelerated synthesis of novel materials. *Nature* **624**(7990), 86–91 (2023)

[55] Fei, Y., Rendy, B., Kumar, R., Dartsi, O., Sahasrabuddhe, H.P., McDermott, M.J., Wang, Z., Szymanski, N.J., Walters, L.N., Milsted, D., *et al.*: Alabos: a python-based reconfigurable workflow management framework for autonomous laboratories. *Digital Discovery* **3**(11), 2275–2288 (2024)

[56] Yang, H., Wu, N.: Ionic conductivity and ion transport mechanisms of solid-state lithium-ion battery electrolytes: A review. *Energy Science & Engineering* **10**(5), 1643–1671 (2022)

[57] Murbach, M.D., Gerwe, B., Dawson-Elli, N., Tsui, L.-k.: impedance. py: A python package for electrochemical impedance analysis. *Journal of Open Source Software* **5**(52), 2349 (2020)

[58] Huang, J., Li, Z., Liaw, B.Y., Zhang, J.: Graphical analysis of electrochemical impedance spectroscopy data in bode and nyquist representations. *Journal of Power Sources* **309**, 82–98 (2016)

[59] Hardy, D.: *The Compound Effect*. Vanguard Press, New York, NY, USA (2011)

[60] Riebesell, J., Goodall, R.E., Benner, P., Chiang, Y., Deng, B., Ceder, G., Asta, M., Lee, A.A., Jain, A., Persson, K.A.: A framework to evaluate machine learning crystal stability predictions. *Nature Machine Intelligence* **7**(6), 836–847 (2025)

[61] Park, Y., Kim, J., Hwang, S., Han, S.: Scalable parallel algorithm for graph neural network interatomic potentials in molecular dynamics simulations. *Journal of chemical theory and computation* **20**(11), 4857–4868 (2024)

[62] Kim, J., Kim, J., Kim, J., Lee, J., Park, Y., Kang, Y., Han, S.: Data-efficient multifidelity training for high-fidelity machine learning interatomic potentials. *Journal of the American Chemical Society* **147**(1), 1042–1054 (2024)

[63] Barroso-Luque, L., Shuaibi, M., Fu, X., Wood, B.M., Dzamba, M., Gao, M., Rizvi, A., Zitnick, C.L., Ulissi, Z.W.: Open materials 2024 (omat24) inorganic materials dataset and models. *arXiv preprint arXiv:2410.12771* (2024)

[64] Ding, K., Yu, J., Huang, J., Yang, Y., Zhang, Q., Chen, H.: Scitoolagent: a knowledge-graph-driven scientific agent for multitool integration. *Nature Computational Science* **5**, 962–972 (2025)

[65] Zaharia, M.A., Chen, A., Davidson, A., Ghodsi, A., Hong, S.A., Konwinski, A., Murching, S., Nykodym, T., Ogilvie, P., Parkhe, M., Xie, F., Zumar, C.: Accelerating the Machine Learning Lifecycle with MLflow. *IEEE Data Eng. Bull.* **41**, 39–45 (2018)

[66] Horton, M.K., Huck, P., Yang, R.X., Munro, J.M., Dwaraknath, S., Ganose, A.M., Kingsbury, R.S., Wen, M., Shen, J.X., Mathis, T.S., *et al.*: Accelerated data-driven materials science with the materials project. *Nature Materials* **24**, 1522–1532 (2025)

[67] Bergerhoff, G., Hundt, R., Sievers, R., Brown, I.D.: The inorganic crystal structure data base. *Journal of Chemical Information and Computer Sciences* **23**(2), 66–69 (1983) <https://doi.org/10.1021/ci00038a003>

[68] Ward, L., Dunn, A., Faghaninia, A., Zimmermann, N.E., Bajaj, S., Wang, Q., Montoya, J., Chen, J., Bystrom, K., Dylla, M., *et al.*: Matminer: An open source toolkit for materials data mining. *Computational Materials Science* **152**, 60–69 (2018)

[69] Huck, P., Gunter, D., Cholia, S., Winston, D., N'Diaye, A., Persson, K.: User applications driven by the community contribution framework mpcontribs in

the materials project. *Concurrency and Computation: Practice and Experience* **28**(7), 1982–1993 (2016)

- [70] Blaiszik, B., Chard, K., Pruyne, J., Ananthakrishnan, R., Tuecke, S., Foster, I.: The materials data facility: data services to advance materials science research. *Jom* **68**(8), 2045–2052 (2016)
- [71] Saal, J.E., Kirklin, S., Aykol, M., Meredig, B., Wolverton, C.: Materials design and discovery with high-throughput density functional theory: the open quantum materials database (oqmd). *Jom* **65**, 1501–1509 (2013)
- [72] Therrien, F., Haibeh, J.A., Sharma, D., Hendley, R., Mungai, L.W., Sun, S., Tchagang, A., Su, J., Huberman, S., Bengio, Y., et al.: Obelix: A curated dataset of crystal structures and experimentally measured ionic conductivities for lithium solid-state electrolytes. arXiv preprint arXiv:2502.14234 (2025)
- [73] Chen, J., Huang, X., Hua, C., He, Y., Schwaller, P.: A multi-modal transformer for predicting global minimum adsorption energy. *Nature Communications* **16**(1), 3232 (2025)
- [74] Chen, J., Huang, X., Hua, C., He, Y., Schwaller, P.: Adsigt: Graph transformer for predicting global minimum adsorption energy. In: NeurIPS 2023 AI for Science Workshop (2023)
- [75] Chen, J., Huang, X., Hua, C., He, Y., Schwaller, P.: AdsMT: Multi-modal Transformer for Predicting Global Minimum Adsorption Energy. Figshare. Figshare (2024). <https://doi.org/10.6084/m9.figshare.25966573.v1> . <https://doi.org/10.6084/m9.figshare.25966573.v1>
- [76] Richards, W.D., Miara, L.J., Wang, Y., Kim, J.C., Ceder, G.: Interface stability in solid-state batteries. *Chemistry of Materials* **28**(1), 266–273 (2016)
- [77] Xiao, Y., Wang, Y., Bo, S.-H., Kim, J.C., Miara, L.J., Ceder, G.: Understanding interface stability in solid-state batteries. *Nature Reviews Materials* **5**(2), 105–126 (2020)
- [78] Gaultois, M.W., Sparks, T.D., Borg, C.K., Seshadri, R., Bonificio, W.D., Clarke, D.R.: Data-driven review of thermoelectric materials: performance and resource considerations. *Chemistry of Materials* **25**(15), 2911–2920 (2013)
- [79] Bartel, C.J., Trewartha, A., Wang, Q., Dunn, A., Jain, A., Ceder, G.: A critical examination of compound stability predictions from machine-learned formation energies. *npj computational materials* **6**(1), 97 (2020)
- [80] Davies, D.W., Butler, K.T., Jackson, A.J., Skelton, J.M., Morita, K., Walsh, A.: Smact: Semiconducting materials by analogy and chemical theory. *Journal of Open Source Software* **4**(38), 1361 (2019)

[81] Jain, A., Ong, S.P., Hautier, G., Chen, W., Richards, W.D., Dacek, S., Cholia, S., Gunter, D., Skinner, D., Ceder, G., et al.: Commentary: The materials project: A materials genome approach to accelerating materials innovation. *APL materials* **1**(1) (2013)

[82] Bradshaw, S., Brazil, E., Chodorow, K.: *MongoDB: the Definitive Guide: Powerful and Scalable Data Storage*. O'Reilly Media, Inc., Sebastopol, CA, USA (2019)

[83] Landrum, G.: *Rdkit documentation. Release 1(1-79)*, 4 (2013)

[84] Ward, L., Agrawal, A., Choudhary, A., Wolverton, C.: A general-purpose machine learning framework for predicting properties of inorganic materials. *npj Computational Materials* **2**(1), 1–7 (2016)

[85] Ganose, A.M., Jain, A.: Robocrystallographer: automated crystal structure text descriptions and analysis. *MRS Communications* **9**(3), 874–881 (2019)

[86] Hart, G.L., Forcade, R.W.: Algorithm for generating derivative structures. *Physical Review B—Condensed Matter and Materials Physics* **77**(22), 224115 (2008)

[87] Hart, G.L., Forcade, R.W.: Generating derivative structures from multilattices: Algorithm and application to hcp alloys. *Physical Review B—Condensed Matter and Materials Physics* **80**(1), 014120 (2009)

[88] Hart, G.L., Nelson, L.J., Forcade, R.W.: Generating derivative structures at a fixed concentration. *Computational Materials Science* **59**, 101–107 (2012)

[89] Morgan, W.S., Hart, G.L., Forcade, R.W.: Generating derivative superstructures for systems with high configurational freedom. *Computational Materials Science* **136**, 144–149 (2017)

[90] Togo, A., Shinozaki, K., Tanaka, I.: Spglib: a software library for crystal symmetry search. *Science and Technology of Advanced Materials: Methods* **4**(1), 2384822 (2024)

[91] Bannwarth, C., Ehlert, S., Grimme, S.: Gfn2-xtb—an accurate and broadly parametrized self-consistent tight-binding quantum chemical method with multipole electrostatics and density-dependent dispersion contributions. *Journal of chemical theory and computation* **15**(3), 1652–1671 (2019)

[92] Neese, F.: The orca program system. *Wiley Interdisciplinary Reviews: Computational Molecular Science* **2**(1), 73–78 (2012)

[93] Larsen, A.H., Mortensen, J.J., Blomqvist, J., Castelli, I.E., Christensen, R., Dułak, M., Friis, J., Groves, M.N., Hammer, B., Hargus, C., et al.: The atomic

simulation environment—a python library for working with atoms. *Journal of Physics: Condensed Matter* **29**(27), 273002 (2017)

- [94] Thompson, A.P., Aktulga, H.M., Berger, R., Bolintineanu, D.S., Brown, W.M., Crozier, P.S., In't Veld, P.J., Kohlmeyer, A., Moore, S.G., Nguyen, T.D., *et al.*: Lammps-a flexible simulation tool for particle-based materials modeling at the atomic, meso, and continuum scales. *Computer physics communications* **271**, 108171 (2022)
- [95] Batatia, I., Kovacs, D.P., Simm, G., Ortner, C., Csányi, G.: Mace: Higher order equivariant message passing neural networks for fast and accurate force fields. *Advances in neural information processing systems* **35**, 11423–11436 (2022)
- [96] Brunken, C., Peltre, O., Chomet, H., Walewski, L., McAuliffe, M., Heyraud, V., Attias, S., Maarand, M., Khanfir, Y., Toledo, E., *et al.*: Machine learning interatomic potentials: library for efficient training, model development and simulation of molecular systems. *arXiv preprint arXiv:2505.22397* (2025)
- [97] Kwon, W., Li, Z., Zhuang, S., Sheng, Y., Zheng, L., Yu, C.H., Gonzalez, J., Zhang, H., Stoica, I.: Efficient memory management for large language model serving with pagedattention. In: *Proceedings of the 29th Symposium on Operating Systems Principles*, pp. 611–626 (2023)
- [98] Chhikara, P., Khant, D., Aryan, S., Singh, T., Yadav, D.: Mem0: Building production-ready ai agents with scalable long-term memory. *arXiv preprint arXiv:2504.19413* (2025)
- [99] Halter, D., *et al.*: Jedi: an awesome auto-completion, static analysis and refactoring library for python. Online document <https://jedi.readthedocs.io> (2022)
- [100] Ji, Z., Lee, N., Frieske, R., Yu, T., Su, D., Xu, Y., Ishii, E., Bang, Y.J., Madotto, A., Fung, P.: Survey of hallucination in natural language generation. *ACM computing surveys* **55**(12), 1–38 (2023)
- [101] Huang, X., Deng, B., Zhong, P., Kaplan, A., Persson, K., Ceder, G.: Materials Project Trajectory Dataset of r2SCAN (MP-r2SCAN). Figshare. Figshare (2025). <https://doi.org/10.6084/m9.figshare.28245650.v2> . [https://figshare.com/articles/dataset/Materials\\_Project\\_Trajectory\\_Dataset\\_of\\_r\\_2\\_SCAN\\_MP\\_r\\_2\\_SCAN\\_28245650](https://figshare.com/articles/dataset/Materials_Project_Trajectory_Dataset_of_r_2_SCAN_MP_r_2_SCAN_28245650)
- [102] Kovács, D.P., Moore, J.H., Browning, N.J., Batatia, I., Horton, J.T., Pu, Y., Kapil, V., Witt, W.C., Magdau, I.-B., Cole, D.J., *et al.*: Mace-off: Short-range transferable machine learning force fields for organic molecules. *Journal of the American Chemical Society* **147**(21), 17598–17611 (2025)